Goodput-Based Link Resource Adaptation for Reliable Packet Transmissions in BIC-OFDM Cognitive Radio Networks

Riccardo Andreotti[1], Ivan Stupia[2], Vincenzo Lottici[1],
Filippo Giannetti[1], and Luc Vandendorpe[2]

Abstract

Cognitive radio (CR) stands out as a potential cornerstone to break the spectrum gridlock through enabling the coexistence of licensed (primary) and unlicensed (secondary) users in the same bandwidth. This paper deals with a novel link resource adaptation (LRA) strategy to be applied in CR scenarios for reliable packet transmissions based on bit interleaved coded orthogonal frequency division multiplexing (BIC-OFDM). We first formulate the power allocation (PA) problem constrained by both the available power at the secondary transmitter (ST) and the interference tolerable at the primary receivers, aimed at maximizing the offered layer 3 data rate, i.e., the goodput (GP) metric. Then, we derive the optimal PA strategy resorting to the customary Lagrangian dual decomposition (LDD) technique, which, however, like many other conventional numerical methods, exhibits several drawbacks, such as slow convergence and need for parameter tuning. These restrictions are circumvented through the development of a novel iterative yet simple PA algorithm, referred to as successive set reduction (SSR) approach, whose optimality conditions are analytically demonstrated by resorting to the Quasi Variational Inequality (QVI) framework. Based on this PA algorithm, an adaptive modulation and coding (AMC) scheme at the ST is eventually derived. Simulation results over a realistic scenario corroborate the effectiveness of the proposed SSR-based AMC algorithm, highlighting the GP improvements over non-adaptive LRA techniques, besides a remarkable complexity reduction w.r.t. conventional numerical methods.

Parts of this paper were presented at the Joint WIC/IEEE SP Symp. on Information Theory and Signal Processing in the Benelux (WICSP) in May 2011.

[1]Department of Information Engineering, University of Pisa, I-56122 Pisa, Italy. Email: {vincenzo.lottici,filippo.giannetti}@iet.unipi.it

[2]Université Catholique de Louvain, B-1348 Louvain-la-Neuve, Belgium.

Index Terms

Automatic repeat request (ARQ), bit-interleaved coded modulation, orthogonal frequency division multiplexing (OFDM), goodput, power allocation, convex optimization, quasi variational inequality.

I. INTRODUCTION

Cognitive radio networks have recently been gaining an ever increasing interest as an effective way to tackle the problem of resource scarcity and inefficiency in the frequency spectrum utilization [1], [2]. Frequency-agile cognitive radios (CRs), employed by unlicensed users, or secondary users (SUs), are the key to this novel radio access paradigm. In fact, after querying a geo-location database or sensing the radio environment [3], such devices adapt their parameters to transmit over segments of spectrum actually owned by licensed users, or primary users (PUs), without causing harmful interference to the latter [4], [5].

Relation to Prior Work. In order to address the above issues, a considerable effort has been devoted on optimizing the performance of the secondary link while guaranteeing coexistence with the primary network. In [6], orthogonal frequency division multiplexing (OFDM) and multi-antennas are exploited to achieve a trade-off between the benefits of spatial multiplexing for SU transmissions and the interference level caused at the PU receivers. In [7], the optimal solution for the power allocation (PA) problem across the OFDM bandwidth is derived by maximizing the secondary link capacity, under limitations on the out-of-band interference to PUs operating on adjacent bands. It also proposes a low-complexity suboptimal approach, called step-ladder (SL) PA, based on the principle that more power shall be loaded on the subcarriers farther from the PU bands. In [8], the same problem is suitably extended such that the constraints about the in-band interference and the available transmit power are taken into consideration. Resource allocation schemes in OFDMA cognitive radio networks are considered in [9] and [10], wherein the sum rate maximization problem is addressed for the single and multi-cell case, respectively.

On the other side, in up-to-date wireless standards such as WiMAX and 3GPP/LTE, the emerging platform is OFDM signaling in combination with a number of advanced features that provide reliable and efficient data packet transmission over harsh fading channels. Among these, we mention here: *i*) efficient channel coding techniques, like the bit-interleaved coded modulation (BICM) [11]; *ii*) automatic repeat request (ARQ) protocol [12]; *iii*) link resource adaptation (LRA) [13], consisting in the adaptation of transmission parameters, such as power-per-subcarrier, modulation order and coding rate, to current channel and operating conditions. In this scenario, information-theoretic performance limits, which rely on ideal assumptions like Gaussian inputs and infinite length codebooks, can reveal inadequate to give a reliable picture of the actual

link performance when practical modulation and coding is applied.

Motivation of the Proposed Approach and Contribution. The above facts fully motivate the adoption of the number of information bits delivered in error-free packets per unit of time [14], [15], or goodput (GP) for short, as a performance metric capable of taking into account the ARQ mechanism as well as the effect of practical modulation and coding schemes. As demonstrated in [16], the estimate of the goodput performance done at the transmitter, named expected goodput (EGP), properly describes the characteristics of the above mentioned system and represents an effective objective function for the LRA problem we are addressing. As a further step to keep complexity at affordable levels, the analytical expression of the EGP is then derived by resorting to the concept of effective SNR mapping (ESM), which yields a scalar value, named effective SNR (ESNR), that uniquely maps the performance of the system at hand into a packet error rate (PER) value [17]. In particular, we adopt the ESM technique based on the cumulant moment generating function of the log-likelihood metrics at the input of the soft decoder, or κESM for short, as recently proposed in [16]. As a matter of fact, it entails several advantages like, among the others, improved performance compared with the conventional exponential-based ESM model, and similar accuracy as the mutual-information-based ESM model, while offering a modulation model with a convex mapping function of the PA coefficients [16]. Other works on LRA for goodput optimization can be found in [14], [15], where hard Viterbi decoding is considered, and in [18] where the PER is derived in a cognitive context, assuming, however, ideal Gaussian codebooks and thus estimating the channel outage probability due to outdated channel state information.

Several original features characterize our contribution. First, the PA problem for goodput optimization in a point-to-point link between a BIC-OFDM secondary transmitter and its receiver is formulated as an optimization problem (OP) under constraints on both the available transmit power and the interference caused to the PUs. This OP is demonstrated to be convex and can be numerically solved through conventional numerical methods, such as the Lagrangian dual decomposition (LDD) technique [19], [20]. However, in order to circumvent the drawbacks of LDD, such as slow convergence and need for parameter tuning, we turn to the Quasi Variational Inequality (QVI) [21], [22]. The latter is a powerful tool, applied to problems such as generalized Nash equilibria and Mathematical Program with Equilibrium Constraints (see [22], [23] and the references therein), which enables the existence proof of solutions and provides guidelines for algorithmic design. Within the QVI framework, we develop then a novel iterative yet simple approach for solving the OP, referred to as successive set reduction (SSR), wherein the constrained PA problem is split into elementary subproblems. We also prove its equivalence with the original PA problem. Finally, we show that the fully heuristic version of the PA algorithm for the PER minimization of a coalition of SUs, derived in [24], [25] by means of geometrical considerations based on the extreme point criterion, belongs

to the proposed framework and its optimality condition is here analytically derived. As a by-product of the SSR algorithm, a simple adaptive modulation and coding (AMC) scheme is eventually formalized, showing remarkable gains compared with non-adaptive PA techniques as the SL-PA in [7]. In fact, since there is no other work dealing with the proposed objective function, the latter represents a fair comparison because it relies on the constraints of the OP and not on the specific objective function.

Organization. The rest of the paper is organized as follows. In Sect. II we describe the cognitive BIC-OFDM scenario and then we define in Sect. III the link resource adaptation problem. Sections IV and V solve the power allocation problem via conventional LDD method and applying the proposed approach, respectively. Finally, Sect. VI is devoted to evaluate performance via computer simulations over typical wireless channels, followed in Sect. VII by some concluding remarks.

Notations. Matrices are in upper case bold while column vectors are in lower case bold; $(\cdot)^{\mathrm{T}}$ denotes the transpose of a matrix or a vector; calligraphic mathematical symbols (e.g., $\mathcal{A}$) denote sets; $\prod_i \mathcal{X}_i$ denotes the Cartesian product of the sets $\mathcal{X}_i$; $\mathrm{diag}(\cdot)$ converts an $N \times 1$ vector into the main diagonal of an $N \times N$ matrix; $\mathcal{CN}(0, \sigma^2)$ denotes the set of the zero-mean complex-valued Gaussian-distributed random variables (RVs) having variance σ^2; $\mathrm{E}_x\{\cdot\}$ denotes statistical expectation w.r.t. to the RV x; $\inf_{x \in \mathcal{X}} F(x)$ denotes the infimum of $F(x)$ over $\mathcal{X}$; $\succ$ and $\succeq$ denote the elementwise greater and greater or equal relations, respectively; the gradient of the function $F(\mathbf{x})$ evaluated in $\overline{\mathbf{x}}$ is given by $\nabla_{\mathbf{x}} F(\overline{\mathbf{x}}) \triangleq [\frac{\partial F}{\partial x_1}, \cdots, \frac{\partial F}{\partial x_{|\mathbf{x}|}}]^{\mathrm{T}}\Big|_{\mathbf{x}=\overline{\mathbf{x}}}$; $\nabla_{\mathbf{x}} \mathbf{F}(\overline{\mathbf{x}})$ denotes the gradient of each component of the vector $\mathbf{F}$, i.e., $\nabla_{\mathbf{x}} \mathbf{F}(\overline{\mathbf{x}}) \triangleq \left[\nabla_{\mathbf{x}} F_1(\overline{\mathbf{x}})^{\mathrm{T}}, \cdots, \nabla_{\mathbf{x}} F_{|\mathbf{F}|}(\overline{\mathbf{x}})^{\mathrm{T}}\right]^{\mathrm{T}}$; finally, $[x]^+ \triangleq \max(0, x)$.

II. System Model Overview

A. Cognitive Scenario

The scenario consists of a BIC-OFDM radio link between a secondary transmitter (ST) and its receiver (SR). Secondary users use the same frequency bands of primary users according to several techniques which depend on the amount of available side information. In practice, due to severe restrictions on the implementation complexity, detailed information such as channel gains or codebooks and messages of PUs will be unlikely available at the ST, which shall instead rely on limited side information only. Thus, coexistence among PUs and SUs is basically ensured by the *underlay* and *interweave* paradigms[1] [4], [5], here briefly recalled.

[1]Please note that in literature there are different definitions of these paradigms. We refer to the definition given, e.g., in [4] that is different from the one given, for example, in [10].

In the underlay paradigm, SUs are allowed to transmit at the same time over the same bands (referred to as grey spaces) used by PUs, called *underlay* PUs (UPUs), as long as the in-band interference caused to them is kept below a certain threshold which depends on the requested PUs quality of service. Clearly, since interference is path-loss dependent, some bands could be forbidden for SUs when they are very close to PUs or to other SUs that are already using those portions of spectrum [4].

In the latter case, SUs should instead look for contiguous unused bands (where unused simply stands for grey space), while ensuring that their out-of-band (OOB) emissions cause a limited interference to the PUs, called *interweave* PUs (IPUs), operating in adjacent bands.

Therefore, adopting the model proposed in [8], the cognitive scenario accounting for both paradigms is described as in Fig. 1. The ST transmits over U bands in the set $\mathcal{B}_{\rm UPU} \triangleq \{B_1, \cdots, B_U\}$ used also by U UPUs. Contiguous to these bands, there are L bands belonging to the set $\mathcal{W}_{\rm IPU} \triangleq \{W_1, \cdots, W_L\}$, where L IPUs are exclusively transmitting. Thus, the overall bandwidth is $B_{\rm tot} \triangleq \sum_{\ell=1}^{L} W_\ell + \sum_{u=1}^{U} B_u$, where secondary transmission occurs over $B \triangleq \sum_{u=1}^{U} B_u$.

B. System Model at Physical and Data Link Layers

The cognitive radio link relies on packet BIC-OFDM signaling. Each packet, represented by the radio-link control (RLC) protocol data unit (PDU), made of $N_{\rm u} = N_{\rm h} + N_{\rm p} + N_{\rm CRC}$ bits, including the header, the payload and the control redundancy check (CRC) sections, of size $N_{\rm h}$, $N_{\rm p}$ and $N_{\rm CRC}$, respectively, is sent to the receiver within T attempts, i.e., the maximum number of ARQ protocol rounds (PRs). At the generic PR t, each RLC-PDU is processed in two steps. In the first, the packet processing step, the RLC-PDU is input to the channel encoder whose coding rate r_t is chosen in the set of punctured rates $\mathcal{D}_r \triangleq \{r_0, \cdots, r_{\min}\}$, where r_0 is the mother code rate and $r_{\min}$ the minimum code rate. The resulting block consists of $N_{{\rm c},t} = N_{{\rm u},t}/r_t$ coded binary symbols, which are are eventually randomly interleaved according to the BICM model. In the second step, i.e., the frame processing, the coded information is mapped onto the physical resources available in the time-frequency grid. Specifically, the ith coded symbol, $1 \leq i \leq N_{{\rm c},t}$, is loaded onto the label of the unit-energy QAM symbol x_{t,n_i,q_i}, which in turn is transmitted within the OFDM symbol q_i, $1 \leq q_i \leq Q$, over the n_i subcarrier, $n_i \in \mathcal{D}_s$, where $\mathcal{D}_s$ is the set collecting the $N = N_{\rm tot}B/B_{\rm tot}$ indexes of the SU active subcarriers out of the total $N_{\rm tot}$ covering the whole bandwidth $B_{\rm tot}$. Multi-level QAM modulation with order uniformly distributed across the N subcarriers is employed, or in other words, the label of the modulation symbol x_{t,n_i,q_i} is made of $m_{t,n_i,q_i} = \bar{m}$ bits belonging to the M-sized set $\mathcal{D}_m = \{2, 4, \cdots, m_{\max}\}$. Subsequently, each block, containing N QAM symbols, undergoes IDFT processing, cyclic prefix insertion and, after digital-to-analog conversion, it is transmitted over a block-

fading frequency-selective channel. Dropping without loss of generality (w.l.g.) the dependence of the QAM symbol x_{t,n_i,q_i} on the indexes $\{i, q_i\}$, the sample received at PR t on the nth subcarrier can be expressed as

$$y_{t,n} = \sqrt{p_{t,n}} h_{t,n} x_{t,n} + w_{t,n} + z_{t,n}, \tag{1}$$

where $h_{t,n}$ is the channel coefficient relevant to the ST-SR link, $p_{t,n} \geq 0$ is the power coefficient, whereas $w_{t,n}$ and $z_{t,n}$ denote the white Gaussian noise contribution and interference, respectively, caused by the PUs, with $w_{t,n} \in \mathcal{CN}(0, {\sigma_{t,n}^{(w)}}^2)$ and $z_{t,n} \in \mathcal{CN}(0, {\sigma_{t,n}^{(z)}}^2)$. Finally, after evaluating the post-processing SNRs $\Gamma_{t,n} \triangleq p_{t,n}\gamma_{t,n}$, $1 \leq n \leq N$, with

$$\gamma_{t,n} = \frac{|h_{t,n}|^2}{{\sigma_{t,n}^{(w)}}^2 + {\sigma_{t,n}^{(z)}}^2}, \tag{2}$$

the receiver performs the soft metric evaluation, followed by de-interleaving and decoding.

C. Power Constraints of the ST

A few constraints arise, at each PR t, that limit the PA distribution $\mathbf{p}_t \triangleq [p_{t,1}, \cdots, p_{t,N}]^{\mathrm{T}}$ that the ST is allowed to allocate on the N subcarriers.

First, designating with P the total power that the ST can spend over the N available subcarriers, $\mathbf{p}_t$ has to comply with

$$f_0(\mathbf{p}_t) \triangleq \sum_{n=1}^{N} p_{t,n} - P \leq 0. \tag{3}$$

Then, considering the in-band interference brought by the ST to the U UPUs described in Sect. II-A, it is reasonable to assume, as in [8], that each PU settles an "interference-free" zone of radius R around itself, wherein any SU transmission is interdicted. This allows PUs to protect themselves from too close SUs, which have to operate so that the interference level caused on the edge of each zone is below a given threshold. This means that the constraints

$$f_u(\mathbf{p}_t) \triangleq \sum_{n:\phi(n)=u} p_{t,n} - T_u \leq 0,\ 1 \leq u \leq U, \tag{4}$$

hold, where $\phi(n) = u$ is an indicator function denoting that subcarrier n used by the ST belongs to the sub-band $B_u \in \mathcal{B}_{\mathrm{UPU}}$ and T_u is the maximum interference (or interference temperature) allowed at the edge of the uth zone scaled by the path loss originated by the ST.

Finally, we focus on the out-of-band interference that can be found within the IPU bands $W_\ell \in \mathcal{W}_{\mathrm{IPU}}$, $1 \leq \ell \leq L$, due to the signal transmitted by the ST. Denoting with $P_\ell(f)$ its spectral density function, the set of feasible PA coefficients $\mathbf{p}_t$ have to be constrained in order to satisfy

$$f_{U+\ell}(\mathbf{p}_t) \triangleq \sum_{n=1}^{N} K_{\ell,n} p_{t,n} - I_\ell \leq 0,\ 1 \leq \ell \leq L, \tag{5}$$

where

$$K_{\ell,n} \triangleq \int_{\Delta f_{n,\ell}-\frac{W_\ell}{2}}^{\Delta f_{n,\ell}+\frac{W_\ell}{2}} P_\ell(f)df, \tag{6}$$

$\Delta f_{n,\ell}$ is the frequency distance between the nth subcarrier and the center of the ℓth IPU band, and I_ℓ is the allowed interference level over that subband, normalized by the path loss of the link ST-uth IPU receiver.

III. Goodput Optimization Problem

This section focuses on the formulation of the optimization problem, whose solution provides a proper setting of transmission parameters, namely, power distribution across the active subcarriers, modulation order and coding rate. To this end, let us refer to the block diagram depicted in Fig. 2, representing an equivalent model of the ARQ-based system described in Sect. II-B. In this model we denoted as $\mathbf{H} \triangleq \mathrm{diag}\{\mathbf{H}_0, \mathbf{H}_1, \cdots, \mathbf{H}_{T-1}\}$, where $\mathbf{H}_t \triangleq \mathrm{diag}\{[h_{t,1}, \cdots, h_{t,N}]\}$, and $\mathbf{X} \triangleq \mathrm{diag}\{\mathbf{X}_0, \mathbf{X}_1, \cdots, \mathbf{X}_{T-1}\}$, where $\mathbf{X}_t \triangleq \mathrm{diag}\{[x_{t,1}, \cdots, x_{t,N}]\}$, the block diagonal matrices containing the channel realizations that could be experienced by the link during T transmissions and the relevant transmitted symbols throughout the T PRs, respectively [2].

In the ideal case, the transmitter has complete "a priori" knowledge of channel status evolution during the time, i.e., the matrix $\mathbf{H}$ is available at the CSI input of the ST in Fig. 2, and thus the transmitter is able to jointly adapt all the parameters to compute $\mathbf{X}$ over the T PRs. Unfortunately, such a joint optimization, though attractive, is clearly impractical, due to the impossibility to reliably predict the whole matrix $\mathbf{H}$ at the beginning of each RLC-PDU transmission. Thus, inspired by [14], we resort instead to a per-round optimization approach based on the *expected goodput* (EGP) metric, which is defined as the ratio of the delivered data payload N_p to the expected transmission time $\mathcal{T}_\mathrm{e}$, i.e., the time that would be necessary to successfully decode the message for the current setting of the transmission parameters. Here, the ST independently adapts, over each branch of the equivalent model in Fig. 2, the power vector $\mathbf{p}_t$ and the transmission mode (TM) $\boldsymbol{\varphi}_t \triangleq \{\mathbf{m}_t, r_t\}$, with $\mathbf{m}_t \triangleq [m_{t,1}, \cdots, m_{t,N}]^\mathrm{T}$, to the current channel conditions $\mathbf{H}_t$ in order to maximize the per-round EGP metric. In particular, at PR t, the expected transmission time can be expressed as

$$\mathcal{T}_\mathrm{e}(\boldsymbol{\varphi}_t, \mathbf{p}_t|\mathbf{H}_t) \triangleq \mathcal{T}_\mathrm{f}(\{\boldsymbol{\varphi}_i\}_{i=0}^{t-1}) + \mathcal{T}_\mathrm{p}(\boldsymbol{\varphi}_t) + \mathcal{T}_\mathrm{p}(\boldsymbol{\varphi}_t)N_\mathrm{e} \tag{7}$$

[2]If the total number of PRs required for transmitting a given RLC-PDU is $T^* < T$, then $\mathbf{X}_t = \mathbf{0}$, for $T^* < t \leq T$.

where $\mathcal{T}_{\mathrm{f}}(\{\boldsymbol{\varphi}_i\}_{i=0}^{t-1})$ represents the time spent in the previous t failed attempts, $\mathcal{T}_{\mathrm{p}}(\boldsymbol{\varphi}_t)$ the time required to transmit the RLC-PDU and

$$N_{\mathrm{e}} \triangleq \chi_{r_t}(\mathbf{m}_t, \mathbf{p}_t|\mathbf{H}_t) \left[1 + \sum_{\substack{\nu= \\ t+1}}^{T-2} \prod_{\substack{i= \\ t+1}}^{\nu} \mathrm{E}_{\mathbf{H}_i} \left\{ \chi_{r_t}(\mathbf{m}_t, \mathbf{p}_t, |\mathbf{H}_i) \right\} \right] \tag{8}$$

the expected number of retransmissions after PR t, being $\chi_{r_t}(\mathbf{m}_t, \mathbf{p}_t|\mathbf{H}_i)$ the packet error probability at PR i when adopting coding rate r_t along with bit and power distribution $\mathbf{m}_t$ and $\mathbf{p}_t$, respectively. Even if appealing, this formulation requires however the knowledge of the channel's probability density function at the ST for all the possible scenarios, which is a problematic assumption in most cases of interest. Thus, we propose a modified version of the EGP metric obtained by substituting the expectation on the future channel conditions with the current channel status, i.e., replacing $\mathrm{E}_{\mathbf{H}_i} \{\chi_{r_t}(\mathbf{m}_t, \mathbf{p}_t, |\mathbf{H}_i)\}$, $t < i < T$, with $\chi_{r_t}(\mathbf{m}_t, \mathbf{p}_t, |\mathbf{H}_t)$. Accordingly, at each PR, the setting of the transmission parameters $\{\mathbf{p}_t, \boldsymbol{\varphi}_t\}$ is the one maximizing the modified EGP metric

$$\zeta_t(\boldsymbol{\varphi}_t, \mathbf{p}_t) \triangleq \frac{N_{\mathrm{p}}}{\mathcal{T}_{\mathrm{p}}(\boldsymbol{\varphi}_t)\varsigma_{r_t}(\mathbf{m}_t, \mathbf{p}_t) + \mathcal{T}_{\mathrm{f}}(\{\boldsymbol{\varphi}_i\}_{i=0}^{t-1})}, \tag{9}$$

where, solving (8),

$$\varsigma_{r_t}(\mathbf{m}_t, \mathbf{p}_t) \triangleq 1 + \frac{1 - \chi_{r_t}(\mathbf{m}_t, \mathbf{p}_t|\mathbf{H}_t)^{T-t-1}}{1 - \chi_{r_t}(\mathbf{m}_t, \mathbf{p}_t|\mathbf{H}_t)}. \tag{10}$$

Let us note that our objective function is equivalent to the EGP we would have assuming that the packet experiences the current channel conditions $\mathbf{H}_t$ throughout its possible future retransmissions (long term static channel assumption). This per-round optimization is performed until the packet is successfully received, or the PR limit T reached. From now on, w.l.g. the dependence on the PR index t will be dropped for simplicity. The probability $\chi_r(\mathbf{m}, \mathbf{p})$ can be efficiently evaluated by exploiting the effective SNR (ESNR) mapping technique [17]. This method consists in simply compressing the SNRs $\boldsymbol{\gamma} \triangleq [\gamma_1, \cdots, \gamma_N]^{\mathrm{T}}$, the TM $\boldsymbol{\varphi}$ and the PA $\mathbf{p}$ into a scalar SNR, i.e., the ESNR value, that provides a reliable prediction of the system performance. More formally, we will adhere to the κESM model as proposed in [16] which has been shown to reliably match the scenario at hand. Accordingly, the ESNR $\gamma(\mathbf{m}, \mathbf{p})$ is such that

$$\chi_{r,\mathrm{AWGN}}[\gamma(\mathbf{m}, \mathbf{p})] = \chi_r(\boldsymbol{\gamma}; \mathbf{m}, \mathbf{p}), \tag{11}$$

where $\chi_{r,\mathrm{AWGN}}[\gamma(\mathbf{m}, \mathbf{p})]$ is the performance (computed off-line) of an equivalent coded binary system operating over an additive white Gaussian noise (AWGN) channel. In [16], it is shown that

$$\gamma(\mathbf{m}, \mathbf{p}) \triangleq -\log \left\{ \frac{1}{\sum_{n=1}^{N} m_n} \sum_{n=1}^{N} \Omega_n(m_n, p_n) \right\}, \tag{12}$$

where

$$\Omega_n(m_n, p_n) \triangleq \alpha_n(m_n)\mathrm{e}^{-\frac{p_n}{\rho_n(m_n)}} \tag{13}$$

is the modulation model for the nth subcarrier, with $\frac{1}{\rho_n(m_n)} \triangleq \gamma_n \left[\frac{d_n(m_n)}{2}\right]^2$, $\alpha_n(m_n)$ and $d_n(m_n)$ being known quantity depending on m_n.

Hence, we are left to the EGP-OP, as stated in the sequel.

EGP-OP. The LRA problem, consisting in finding the TM $\boldsymbol{\varphi}$ and the power vector $\mathbf{p}$ which maximizes, at each PR, the EGP subject to the available power and interference constraints, can be written as

$$\begin{aligned} (\boldsymbol{\varphi}^*, \mathbf{p}^*) = & \underset{(\boldsymbol{\varphi}, \mathbf{p})}{\arg\max} \{\zeta(\boldsymbol{\varphi}, \mathbf{p})\} \\ \text{s.t.} \quad & \mathbf{p} \succeq \mathbf{0} \qquad (14.\text{a}) \\ & \boldsymbol{f}(\mathbf{p}) \preceq \mathbf{0} \qquad (14.\text{b}) \\ & \boldsymbol{\varphi} \in \mathcal{D}_{\boldsymbol{\varphi}} \qquad (14.\text{c}) \end{aligned} , \tag{14}$$

where $\boldsymbol{f}(\mathbf{p}) \triangleq [f_0(\mathbf{p}), \cdots, f_{U+L}(\mathbf{p})]^{\mathrm{T}}$ is the $(U+L+1)$-sized vector including the constraints (3)-(5) and $\mathcal{D}_{\boldsymbol{\varphi}}$ is the set of allowed transmission modes. ■

The structure of the EGP-OP (a mixed integer problem) allows to optimally decouple the problem in two parts. First, the optimal PA $\mathbf{p}^*(\boldsymbol{\varphi}_0)$ for a given TM $\boldsymbol{\varphi}_0$ is found, then a simple exhaustive search is done over the finite-size set of the possible TMs to find the pair $\{\mathbf{p}^*(\boldsymbol{\varphi}_0^*), \boldsymbol{\varphi}_0^*\}$ corresponding to the highest EGP value. These issues will be addressed in the following sections.

IV. Optimal Power Allocation

In this section, the PA problem for EGP optimization, based on (14), is formulated and then solved via the well-known dual decomposition method.

A. Formulation of the Power Allocation Problem

The optimal PA distribution solving (14), for a given TM $\boldsymbol{\varphi} = \boldsymbol{\varphi}_0$, is the vector $\mathbf{p}^* \triangleq [p_1^*, \cdots, p_N^*]^{\mathrm{T}}$ that minimizes the numerator of the argument of the logarithm in (12), due to the structure of the EGP objective function $\zeta(\boldsymbol{\varphi}, \mathbf{p})$ in (9); see [16] for additional details. Accordingly, the EGP oriented PA problem (EGOPA-OP) can be reformulated as follows.

EGOPA-OP. Given TM $\boldsymbol{\varphi} = \boldsymbol{\varphi}_0$, the EGP oriented power allocation OP can be formulated as

$$\begin{aligned} \mathbf{p}^* = & \arg\min_{\mathbf{p}} \{\psi(\boldsymbol{\varphi}_0, \mathbf{p})\} \\ \text{s.t.} \quad & \mathbf{p} \succeq \mathbf{0} \qquad (15.\text{a}) \\ & \boldsymbol{f}(\mathbf{p}) \preceq \mathbf{0} \qquad (15.\text{b}) \end{aligned} , \tag{15}$$

where, according to (13), the objective function is expressed as

$$\psi(\boldsymbol{\varphi}_0, \mathbf{p}) \triangleq \sum_{n=1}^{N} \Omega_n(m_n^{(0)}, p_n) = \sum_{n=1}^{N} \alpha_n \mathrm{e}^{-\frac{p_n}{\rho_n}}. \tag{16}$$

■

Let us notice that, for the sake of notational simplicity, in the following we will denote the objective function as $\psi(\mathbf{p})$, dropping the dependence on the TM $\boldsymbol{\varphi}_0$.

B. Lagrangian Dual Decomposition Approach

Since the objective function $\psi(\mathbf{p})$ is convex and the set of constraints (15.a)-(15.b) too, the EGOPA-OP is convex and thus can be optimally solved applying the Lagragian dual decomposition (LDD) technique [19]. Upon denoting as ϑ_m the mth Lagrange multiplier relevant to constraints (15.b) and stacking them into the $(U+L+1)$-sized vector $\boldsymbol{\vartheta} \triangleq [\vartheta_0, \cdots, \vartheta_{U+L}]^{\mathrm{T}}$, the Lagrangian associated with the EGOPA-OP (15) is

$$\Lambda(\boldsymbol{\vartheta}, \mathbf{p}) \triangleq \psi(\mathbf{p}) + \boldsymbol{\vartheta}^{\mathrm{T}} \boldsymbol{f}(\mathbf{p}). \tag{17}$$

Hence, the LDD approach consists of two sub-problems:

S1: the dual problem in order to obtain a lower bound on the optimal value $\psi^* \triangleq \psi(\mathbf{p}^*)$ of the primal problem (15)

$$\boldsymbol{\vartheta}^* = \arg\max_{\boldsymbol{\vartheta} \in \mathcal{D}_{\boldsymbol{\vartheta}}} \{g(\boldsymbol{\vartheta})\}, \tag{18}$$

S2: the determination of the dual function

$$g(\boldsymbol{\vartheta}) = \inf_{\mathbf{p} \in \mathcal{D}_{\mathbf{p}}} \{\Lambda(\boldsymbol{\vartheta}, \mathbf{p})\}, \tag{19}$$

where $\mathcal{D}_{\boldsymbol{\vartheta}} \triangleq \{\boldsymbol{\vartheta} : \vartheta_m \geq 0, 0 \leq m \leq U+L\}$ and $\mathcal{D}_{\mathbf{p}} \triangleq \{\mathbf{p} : p_n \geq 0, 1 \leq n \leq N\}$. We note that the difference between the optimal value ψ^* and the optimal dual value $g^* \triangleq g(\boldsymbol{\vartheta}^*)$, i.e., the duality gap according to the convex analysis is zero, i.e., strong duality holds, thus implying that the primal problem (15) can be equivalently solved by solving the dual problem, as stated in the following proposition.

Theorem 1. In view of the convexity of the EGOPA-OP, the duality gap is zero and the Karush-Kuhn-Tucker (KKT) conditions are sufficient to derive the optimal PA $\mathbf{p}^*$ as

$$p_n^* = \rho_n \left[\log \frac{1}{\vartheta_0^* + \vartheta_{\phi(n)}^* + \sum_{\ell=1}^{L} \vartheta_{U+\ell}^* K_{\ell,n}} - \log \frac{\rho_n}{\alpha_n} \right]^+ \tag{20}$$

$\forall n \in \mathcal{D}_s$, where $\boldsymbol{\vartheta}^*$ is the optimal value of the Lagrange multipliers, ρ_n and α_n are defined in Sec. III, and $\phi(n)$ is the indicator function used in (4).

Proof. See Appendix A. ■

The following remarks about Theorem 1 are now of interest.

1) As specified by the LDD method, the optimal PA solution (20) requires the evaluation of the optimal values about the Lagrange multipliers $\boldsymbol{\vartheta}^*$. Such a (demanding) task can be accomplished numerically (note that a closed-form expression does not exist) applying sub-gradient based updating [20], as summarized in Tab. I. Therein, $\mathbf{p}_0$ denotes the initial setting of the PA coefficients, e.g., $\mathbf{p}_0 \triangleq [0, \cdots, 0]^{\mathrm{T}}$, $\mathbf{p}^{(i)} \triangleq [p_1^{(i)}, \cdots, p_N^{(i)}]^{\mathrm{T}}$ is the latter quantity at the ith iteration, $\boldsymbol{\vartheta}^{(i)} \triangleq [\vartheta_0^{(i)}, \cdots, \vartheta_{U+L}^{(i)}]^{\mathrm{T}}$ contains the Lagrange multipliers at the ith iteration, $\boldsymbol{\xi} = [\xi_0, \cdots, \xi_{U+L}]^{\mathrm{T}}$ is the step-size vector, ε is the maximum convergence error, and $I_{\max}$ is the maximum number of iterations allowed. At the ith iteration, first sub-problem S1 is solved by updating $\boldsymbol{\vartheta}^{(i)}$ using the gradient $\nabla_{\boldsymbol{\vartheta}} \Lambda(\boldsymbol{\vartheta}^{(i)}, \mathbf{p}^{(i)})$, scaled by the step-size $\boldsymbol{\xi}$. Then, the LDD solves sub-problem S2 and updates the optimal PA $\mathbf{p}^{(i)}$ using the closed-form expression (20) and the multipliers $\boldsymbol{\vartheta}^{(i+1)}$ from S1. The procedure is then iterated until convergence is achieved, in view of the strong duality property of the problem at hand [19]. Since a fixed step size is adopted and the norm of the subgradient vector is bounded, the subgradient update method is known to converge to the optimal value within $\|\boldsymbol{\xi}\|_2 G^2$ of accuracy, where $G \geq \|\boldsymbol{f}(\mathbf{p})\|_2$.

2) Moreover, this is obtained at the price of a demanding computational complexity load of $\mathcal{O}(1/\varepsilon^2)$. Further, whenever the problem dimensionality is high (as in our case) it incurs in an extremely slow convergence [20]. The above hard drawbacks will motivate an equivalent yet numerically efficient optimization method, as outlined in Sect. V.

3) The optimal PA offers an interesting multi-level water-filling interpretation [8], [10]. The first term within the square brackets in (20), indeed, is the water level per subcarrier, determined by the available power and interference constraints, whereas the second one is the height of the vessel bottom that depends on the inverse of the SINR.

V. Successive Set Reduction Approach

In this section a novel approach to the PA problem for EGP maximization is formalized. Sections V-A and V-B provide motivations and the formal description of the SSR problem. In Section V-C, resorting to the QVI theory, we show the existence of the SSR solution. In Sections V-D and V-E an iterative algorithm for PA based on the SSR approach is then introduced and some sufficient conditions for optimality under interweave and underlay interference constraints are also discussed. Finally, the AMC algorithm is described.

A. Rationale of the SSR approach.

Unfortunately, conventional numerical methods, such as the LDD method described in previous Sect. IV-B, can lead to extremely slow convergence. Moreover, a careful off-line tuning of the step size $\boldsymbol{\xi}$ and Lagrange multipliers initialization are often required for guaranteeing a fast convergence. Therefore the following subsections present a novel methodology which overcomes these obstacles relying on a different geometric interpretation of the power allocation problem. Actually, differently from the LDD approach, which builds a lower bound of the objective function and operates over a new set of variables defined by the multipliers, the novel proposed method exploits the *monotonicity* property of the objective function $\psi(\mathbf{p})$ to rearrange the original optimization problem as a mathematical program with equilibrium constraints (MPEC)[3] [23]. This goal can be achieved by deriving a splitting rule for the original set of constraints, together with an optimality condition guaranteeing the equivalence between the original problem and the equivalent MPEC-based re-formulation. This design approach provides then an iterative algorithm that, step by step, moves towards a "promising" region (i.e. a reduced set) where to look for the solution. More specifically, thanks to a proper partition of the set of feasible power vectors, each step of the algorithm produces a *closed-form* power increment that decreases more and more the value of the objective function $\psi(\mathbf{p})$, defined in (16), to be minimized. This power increment is obtained by optimizing a properly shifted version of $\psi(\mathbf{p})$ over a reduced set of feasible powers. For this reason, we will refer to this novel methodology as successive set reduction, or SSR for short, and, accordingly, to the relevant iterative algorithm as the SSR algorithm.

B. SSR Approach to the EGP maximization problem

In this subsection, we define the novel SSR approach that offers a solution $\mathbf{p}_J \triangleq \sum_{j=1}^{J} \delta\mathbf{p}_j$, where the power increments $\delta\mathbf{p}_j \triangleq [\delta p_{j,1}, \cdots, \delta p_{j,N}]^{\mathrm{T}}$, $\forall j$, are obtained relying on a proper decomposition of the EGOPA-OP (15) into a set of J subproblems, each of which solved through a simple closed-form equation.

[3]MPEC constitute a special class of mathematical programs where the decision variables satisfy a finite number of constraints together with an equilibrium condition.

First of all, let us define the vectors $\delta\mathbf{p} \triangleq [\delta\mathbf{p}_1^{\mathrm{T}}, \delta\mathbf{p}_2^{\mathrm{T}}, \cdots, \delta\mathbf{p}_J^{\mathrm{T}}]^{\mathrm{T}} \in \Re^{NJ}$ and $\delta\mathbf{p}_{-j} \triangleq [\delta\mathbf{p}_1^{\mathrm{T}}, \cdots, \delta\mathbf{p}_{j-1}^{\mathrm{T}}, \delta\mathbf{p}_{j+1}^{\mathrm{T}}, \cdots, \delta\mathbf{p}_J^{\mathrm{T}}]^{\mathrm{T}} \in \Re^{N(J-1)}$. Thus, introducing the set $\mathcal{J} \triangleq \{1, 2, \cdots, J\}$, the J-dimensional SSR problem can be defined as follows.

Proposition 1: SSR Problem. The vector $\delta\mathbf{p}^* \in \Re^{NJ}$ is the SSR solution if it jointly solves the following optimization problems, tagged as SSR subproblems, $\forall j \in \mathcal{J}$

$$\begin{aligned} \min_{\delta\mathbf{p}_j} \quad & \psi_j(\delta\mathbf{p}_j, \delta\mathbf{p}_{-j}) \\ \text{s.t.} \quad & \delta\mathbf{p}_j \succeq 0 \qquad (21.\text{a}) \\ & u_j(\delta\mathbf{p}_j) \leq 0 \quad (21.\text{b}) \\ & w_j(\delta\mathbf{p}_j, \delta\mathbf{p}_{-j}) \leq 0 \quad (21.\text{c}) \end{aligned} \tag{21}$$

where both u_j and w_j are assumed to be continuously differentiable affine functions (that will be analytically derived in the next section) in the argument $\delta\mathbf{p}_j$ and

$$\psi_j(\delta\mathbf{p}_j, \delta\mathbf{p}_{-j}) \triangleq \sum_{n=1}^{N} \tilde{\alpha}_n(\delta\mathbf{p}_{-j}) \mathrm{e}^{-\frac{\delta p_{j,n}}{\rho_n}} \tag{22}$$

represents the objective function associated to the jth increment, with $\delta\mathbf{p}_0 \triangleq \mathbf{0}$ and

$$\tilde{\alpha}_n(\delta\mathbf{p}_{-j}) \triangleq \alpha_n \left(\prod_{\upsilon=0}^{j-1} \mathrm{e}^{-\frac{\delta p_{\upsilon,n}}{\rho_n}} \right). \tag{23}$$

■

Note that the new objective function in (22) is a properly shifted version of the original objective function (16), while the number of reduced sets J depends on the topology of the original set of the feasible power allocation vectors and on the splitting rule of the original set. The design guidelines for an iterative algorithm producing the reduced sets will be defined in the following sections. Now, let us denote the solution set of the jth SSR subproblem (21) as $\mathcal{S}_j(\delta\mathbf{p}_{-j}) \subset \Re^N$. In the sequel, we will refer to (22) either as $\psi_j(\delta\mathbf{p}_j, \delta\mathbf{p}_{-j})$ or $\psi_j(\delta\mathbf{p})$ at our best convenience. The SSR solution is then the NJ-tuple $\delta\mathbf{p}^*$ such that $\delta\mathbf{p}_j^* \in \mathcal{S}_j(\delta\mathbf{p}_{-j}^*)$ $\forall j \in \mathcal{J}$. Equivalently, a necessary condition for the existence of the solution $\delta\mathbf{p}^*$ to the SSR problem is that there exist some constraint multipliers $\boldsymbol{\lambda} \triangleq [\lambda_1, \lambda_2, \cdots, \lambda_J]^{\mathrm{T}}$ and $\boldsymbol{\mu} \triangleq [\mu_1, \mu_2, \cdots, \mu_J]^{\mathrm{T}}$ such that the KKT systems

$$\nabla_{\delta\mathbf{p}_j} \psi_j(\delta\mathbf{p}_j^*, \delta\mathbf{p}_{-j}^*) + \lambda_j \nabla_{\delta\mathbf{p}_j} w_j(\delta\mathbf{p}_j^*, \delta\mathbf{p}_{-j}^*) + \mu_j \nabla_{\delta\mathbf{p}_j} u_j(\delta\mathbf{p}_j^*) = 0 \tag{24}$$

$$\lambda_j \geq 0, \quad \mu_j \geq 0 \qquad (24.\text{a})$$

$$\mu_j u_j(\delta\mathbf{p}_j^*) = 0 \qquad (24.\text{b})$$

$$\lambda_j w_j(\delta\mathbf{p}_j^*, \delta\mathbf{p}_{-j}^*) = 0 \qquad (24.c)$$

hold $\forall j \in \mathcal{J}$.

Finally, consider the point-to-set map $\mathcal{K}_j : \Re^{N(J-1)} \to \Re^N$, given by

$$\mathcal{K}_j(\delta\mathbf{p}_{-j}) \triangleq \left\{\delta\mathbf{p}_j \in \Re^N : w_j(\delta\mathbf{p}_j, \delta\mathbf{p}_{-j}) \leq 0, \quad u_j(\delta\mathbf{p}_j) \leq 0\right\}. \qquad (25)$$

Since $\psi_j(\delta\mathbf{p}_j, \delta\mathbf{p}_{-j})$ is convex in $\delta\mathbf{p}_j$, a point $\delta\mathbf{p}_j^* \in \Re^N$, is the solution of the jth SSR subproblem if and only if (*minimum principle*) [21]

$$(\delta\mathbf{p}_j - \delta\mathbf{p}_j^*)^{\mathrm{T}} \nabla_{\delta\mathbf{p}_j} \psi_j(\delta\mathbf{p}_j^*, \delta\mathbf{p}_{-j}) \geq 0 \quad \forall \delta\mathbf{p}_j \in \mathcal{K}_j(\delta\mathbf{p}_{-j}). \qquad (26)$$

Interestingly, the latter can be interpreted as an instance of

$$(\delta\mathbf{p} - \delta\mathbf{p}^*)^{\mathrm{T}} F(\delta\mathbf{p}^*) \geq 0 \qquad \forall\, \delta\mathbf{p} \in \mathcal{K}(\delta\mathbf{p}^*). \qquad (27)$$

which is the QVI($\mathcal{K}, F$) problem, where $F(\delta\mathbf{p}) \triangleq [F_1^{\mathrm{T}}(\delta\mathbf{p}), \cdots, F_J^{\mathrm{T}}(\delta\mathbf{p})]^{\mathrm{T}}$: $\Re^{NJ} \to \Re^{NJ}$, with $F_j(\delta\mathbf{p}) \triangleq \nabla_{\delta\mathbf{p}_j} \psi_j(\delta\mathbf{p}_j, \delta\mathbf{p}_{-j})$, and $\mathcal{K}(\delta\mathbf{p}) \triangleq \prod_{j=1}^J \mathcal{K}_j(\delta\mathbf{p}_{-j})$. In the next subsection, we will provide sufficient conditions for such a QVI to have a solution.

C. Existence of the SSR Solution

In order to demonstrate the existence of the solution for the SSR problem, we will pursue an approach analogous to the one proposed in [22] for generalized Nash equilibria, which is specifically tailored for sets $\mathcal{K}_j(\delta\mathbf{p}_{-j})$ that are representable by convex inequalities. However, differently from the generalized Nash equilibrium problem, here the equilibrium condition must be satisfied among the reduced subsets instead of among different competitive players. Thus, we will extend that approach to take into account the particular structure of our problem (27). In particular, as in [22], we will rely on both the well-known Kakutani's fixed-point theorem [21] and the following Sequentially Bounded Constraints Qualification (SBCQ) assumption [23] for each SSR subproblem $j \in \mathcal{J}$.

Definition 1. SBCQ: *for any bounded sequence of vectors* $\{\delta\mathbf{p}_j^{(k)}\} \in \mathcal{S}_j(\delta\mathbf{p}_{-j}^{(k)})$ $\forall k$*, there exists a corresponding bounded sequence* $\{\lambda_j^{(k)}\}$ *of Lagrange multipliers satisfying the* j*th KKT system.*

Remark. Accordingly, for each $\delta\mathbf{p}^{(k)} \triangleq [{\delta\mathbf{p}_1^{(k)}}^{\mathrm{T}}, \cdots, {\delta\mathbf{p}_J^{(k)}}^{\mathrm{T}}]^{\mathrm{T}}$ feasible to (27), KKT multipliers exist for the solution of the jth SSR problem (21), i.e., KKT conditions hold with bounded multipliers on bounded sets.

Let us start by defining the constraint functions u_j and w_j in (21.b) and (21.c), respectively, as

$$u_j(\delta\mathbf{p}_j) \triangleq -1 + \sum_{n=1}^{N} \frac{\delta p_{j,n}}{P_j}, \tag{28}$$

$$w_j(\delta\mathbf{p}_j, \delta\mathbf{p}_{-j}) \triangleq -1 + \sum_{n=1}^{N} \frac{\delta p_{j,n}}{\Theta_{j,n}(\delta\mathbf{p}_{-j})}, \tag{29}$$

where $\Theta_{j,n}(\delta\mathbf{p}_{-j})$ are convex differentiable functions and $\{P_j\}_{j=1}^{J}$ are properly defined positive constant values, and let

$$\mathcal{X}_j \triangleq \left\{\delta\mathbf{p}_j \in \Re^N : u_j(\delta\mathbf{p}_j) \leq 0\right\}, \quad \mathcal{X}_{-j} \triangleq \prod_{\upsilon=1,\upsilon\neq j}^{J} \mathcal{X}_\upsilon \tag{30}$$

be the sets identified only by the constraints depending on $\delta\mathbf{p}_j$. We now summarize in the following theorem some sufficient conditions which guarantee the existence of the QVI solution.

Theorem 2: Solution Existence. Let $F : \Re^{NJ} \to \Re^{NJ}$ be a point-to-point map and let $\mathcal{K} : \Re^{NJ} \to \Re^{NJ}$ a point-to-set map such that

a) for each $\delta\mathbf{p}_{-j} \in \mathcal{X}_{-j}$ the set $\mathcal{K}_j(\delta\mathbf{p}_{-j})$ is nonempty, $\forall j \in \mathcal{J}$ (feasibility assumption),

b) $\Theta_{j,n}(\delta\mathbf{p}_{-j}) > 0$, $\forall j \in \mathcal{J}$ and $\forall n \in \mathcal{D}_s$,

c) the set $\mathcal{X}_j$ is nonempty and bounded, $\forall j \in \mathcal{J}$ (compactness assumption),

then the QVI$(\mathcal{K}, F)$ solution is ensured. ■

Proof. At first, note that the SSR subproblem defined as in (21), parameterized in $\delta\mathbf{p}_{-j}$, is convex in $\delta\mathbf{p}_j$. Hence, being $\Theta_{j,n}(\delta\mathbf{p}_{-j}) > 0$ $\forall n \in \mathcal{D}_s$ and $\forall j \in \mathcal{J}$ and thus belonging $\delta\mathbf{p}_j$ to a bounded set, there always exists a bounded pair (λ_j, μ_j). This means that the SBCQ assumption holds.
Now, exploiting assumption c) we can deduce that

$$\mathcal{X} \triangleq \prod_{j=1}^{J} \mathcal{X}_j \tag{31}$$

is a compact, nonempty and convex subset of $\Re^{NJ}$. Hence, the mapping defined as

$$\Phi(\delta\mathbf{p}) \triangleq \prod_{j=1}^{J} \mathcal{S}_j(\delta\mathbf{p}_{-j}) \tag{32}$$

is a nonempty, compact and convex subset of $\mathcal{X}$. Even looking at (32), since for a given $\delta\mathbf{p}_{-j}$ the original optimization problem is convex, the set $\mathcal{S}_j$ is a singleton. It follows that the QVI($\mathcal{K}$, F) has solution given that the set-valued map Φ has a fixed point, i.e., $\delta\mathbf{p}^* = \Phi(\delta\mathbf{p}^*)$. Then, under the Kakutani's fixed point theorem, demonstrating the existence of the SSR solution amounts to show that Φ is a closed point-to-set

map, according to the following definition [26].

Definition 2. *The mapping Φ is closed at a point $\delta\bar{\mathbf{p}} \triangleq [\delta\bar{\mathbf{p}}_1^{\mathrm{T}}, \cdots, \delta\bar{\mathbf{p}}_J^{\mathrm{T}}]^{\mathrm{T}} \in \mathcal{X}$ if, given two sequences $\{\delta\mathbf{p}^{(k)}\}$ and $\{\delta\mathbf{v}^{(k)}\}$ belonging to $\mathcal{X}$, with $\delta\mathbf{p}^{(k)} \triangleq [\delta\mathbf{p}_1^{(k)^{\mathrm{T}}}, \cdots, \delta\mathbf{p}_J^{(k)^{\mathrm{T}}}]^{\mathrm{T}}$ and $\delta\mathbf{p}^{(k)} \triangleq [\delta\mathbf{v}_1^{(k)^{\mathrm{T}}}, \cdots, \delta\mathbf{v}_J^{(k)^{\mathrm{T}}}]^{\mathrm{T}}$, such that*

$$\lim_{k\to\infty} \delta\mathbf{p}_j^{(k)} = \delta\bar{\mathbf{p}}_j, \qquad \lim_{k\to\infty} \delta\mathbf{v}_j^{(k)} = \delta\bar{\mathbf{v}}_j \tag{33}$$

and $\delta\mathbf{v}_j^{(k)} \in \mathcal{S}_j(\delta\mathbf{p}_{-j}^{(k)})$ $\forall k$ and $\forall j$, then it follows that $\delta\bar{\mathbf{v}}_j \in \mathcal{S}_j(\delta\bar{\mathbf{p}}_{-j})$.

As demonstrated in Appendix B, under the SBCQ, there always exist two bounded multipliers vectors $\boldsymbol{\lambda}$ and $\boldsymbol{\mu}$ such that $\delta\bar{\mathbf{v}}_j \in \mathcal{S}_j(\delta\bar{\mathbf{p}}_{-j})$, $\forall j \in \mathcal{J}$, thus demonstrating the existence of the SSR solution. ■

D. SSR algorithm

We now reformulate the EGP maximization problem in a simpler equivalent form obtained through the SSR approach. To accomplish this task, we first derive the condition under which the power vector

$$\mathbf{p}_J \triangleq \sum_{j=1}^{J} \delta\mathbf{p}_j^* = [p_{J,1}, \cdots, p_{J,N}]^{\mathrm{T}}, \tag{34}$$

referred to as SSR power allocation (SSR-PA) and obtained as the combination of the single components of the SSR solution, solves the EGOPA-OP (15).

First of all, let us note that the formulation of the SSR subproblem (21) is analogous to the PA problem for EGP optimization originally proposed in [16] for a non-cognitive context. Assuming, w.l.g., that in (29) and (28) $P_j \geq \Theta_{j,n}(\delta\mathbf{p}_{-j})$, $\forall n \in \mathcal{D}_s$, the following theorem can be stated.

Theorem 3. The solution of the jth SSR subproblem (21), $\delta\mathbf{p}_j^* \triangleq [\delta p_{j,1}^*, \cdots, \delta p_{j,N}^*]^{\mathrm{T}}$, $\forall j \in \mathcal{J}$, can be expressed by

$$\delta p_{j,n}^* = \rho_n \left[\frac{1 + \sum\limits_{i=1}^{N} \tilde{\rho}_{j,i} \log\left(\frac{\tilde{\rho}_{j,i}}{\tilde{\alpha}_{j,i}} \frac{\tilde{\alpha}_{j,n}}{\tilde{\rho}_{j,n}} \right)}{\sum\limits_{k=1}^{N} \tilde{\rho}_{j,k}} \right]^{+} \quad \forall n \in \mathcal{D}_s, \tag{35}$$

where $\tilde{\rho}_{j,n} \triangleq \frac{\rho_n}{\Theta_{j,n}}$ and, for the sake of readability, the dependence of $\Theta_{j,n}$ and $\tilde{\alpha}_{j,n}$ to $\delta\mathbf{p}_{-j}$ is omitted.

Proof. See Appendix C. ■

It is then possible to exploit the expression of the jth SSR solution, providing a simple way to compute the SSR-PA. Given a fixed j, let define the subcarrier indices set $\mathcal{N}_j$ as

$$\mathcal{N}_j \triangleq \{n \in \mathcal{D}_s : \delta p_{j,n} \neq 0\}, \ \ \forall j \in \mathcal{J}, \tag{36}$$

so that, jointly exploiting (23), (34) and (35), we get the SSR-PA

$$\frac{p_{J,n}}{\rho_n} = \log\left(\frac{1}{\lambda_J}\right) + \log\left(\Theta_{J,n}\right) - \log\left(\frac{\rho_n}{\alpha_n}\right) \quad \forall n \in \mathcal{N}_J \tag{37}$$

with

$$\log\left(\frac{1}{\lambda_J}\right) = \frac{1 + \sum\limits_{i\in\mathcal{N}_J} \frac{1}{\Theta_{J,n}} \left[\rho_i \log\left(\frac{\rho_i}{\alpha_i\, \Theta_{J,n}}\right) + p_{J-1,i}\right]}{\sum\limits_{k\in\mathcal{N}_J} \frac{\rho_k}{\Theta_{J,k}}}. \tag{38}$$

It is now worth to highlight the following result.

cEGOPA-OP. The SSR-PA $\mathbf{p}_J$ given in (37) is also the solution to the following convex optimization problem, tagged as cost-based EGOPA-OP or cEGOPA-OP:

$$\begin{aligned} \min_{\mathbf{p}} \quad & \psi(\mathbf{p}) + \lambda_J\, C_J(\mathbf{p}) \\ \text{s.t.} \quad & \mathbf{p} \succeq 0 \end{aligned} \tag{39}$$

where

$$C_J(\mathbf{p}) \triangleq \sum_{n=1}^{N} \frac{p_n}{\Theta_{J,n}} - 1 \tag{40}$$

plays the role of a linear cost function.

The equivalence can be easily verified by solving the KKT system of the cEGOPA-OP (39) and noting that the gradient of the cost function is a constant vector given by $\nabla_{\mathbf{p}} C_J(\mathbf{p}_J) = [1/\Theta_{J,1}, 1/\Theta_{J,2}, \cdots, 1/\Theta_{J,N}]^{\mathrm{T}}$. Interestingly, in the objective function of (39) we meet again the objective function $\psi(\mathbf{p})$ of the EGOPA-OP (15).

Comparing (37) with (20), we infer that, in general, the SSR approach does not provide solutions to (15). An interesting question is whether one can design the reduced set constraints so that the SSR solution coincides with the optimal power allocation. The answer is given by the following theorem.

Theorem 4: Optimality Condition. Let the set $\mathcal{I}(\mathbf{p}_J) \triangleq \{i : f_i(\mathbf{p}_J) = 0\}$ be the non-empty set of indices associated to the constraints $f_i(\mathbf{p}_J)$ that hold with equality in $\mathbf{p} = \mathbf{p}_J$ and assume that $\mathbf{p}_J$ is a feasible vector to the EGOPA-OP (15) and the following condition is satisfied

$$\frac{\partial C_J(\mathbf{p}_J)}{\partial p_n} = \frac{1}{\Theta_{J,n}} = \frac{A}{\sigma_{\phi(n)} + \mu \sum\limits_{i\in\mathcal{I}(\mathbf{p}_J),\, i>U} K_{i,n}}, \quad \forall n \in \mathcal{N}_J \tag{41}$$

where $\sigma_{\phi(n)}$, μ, A are constant coefficients, such that $\sigma_{\phi(n)} \geq 0$, $\mu \geq 0$, $\sigma_{\phi(n)} + \mu > 0$, and $A > 0$.
Then, the power vector $\mathbf{p}_J$ obtained through (34) represents the optimal solution of EGOPA-OP. ■

Proof. By writing the KKT system associated to the cEGOPA-OP (39) and comparing it with the KKT condition (48) in Appendix A of the EGOPA-OP, we obtain that $\mathbf{p}_J$ is the solution of the original problem if and only if it exists a positive vector $\boldsymbol{\vartheta}$ such that

$$\sum_{i\in\mathcal{I}(\mathbf{p}_J)} \vartheta_i \nabla_{\mathbf{p}} f_i(\mathbf{p}_J) = \lambda_J \nabla_{\mathbf{p}} C(\mathbf{p}_J) \tag{42}$$

where $\vartheta_i = 0$, $\forall i \notin \mathcal{I}(\mathbf{p}_J)$. In other words, we can claim that $\mathbf{p}_J$ is the solution of our PA problem if $\nabla_{\mathbf{p}} C(\mathbf{p}_J)$ belongs to the convex cone generated by the vectors $\{\nabla_{\mathbf{p}} f_i(\mathbf{p}_J)\}_{i\in\mathcal{I}(\mathbf{p}_J)}$. From the Farka's Lemma, [19], this is true if it does not exist a vector $\mathbf{y} \in \Re^N$ such that

$$\mathrm{Z}_J^{\mathrm{T}}\mathbf{y} \geq 0 \;\; (43.\mathrm{a}) \;\text{ and }\; \nabla_{\mathbf{p}} C(\mathbf{p}_J)^{\mathrm{T}}\mathbf{y} < 0 \;\; (43.\mathrm{b}), \tag{43}$$

with $\mathrm{Z}_J \triangleq \left[\nabla_{\mathbf{p}} f_{i_1}(\mathbf{p}_J)^{\mathrm{T}}, \cdots, \nabla_{\mathbf{p}} f_{i_M}(\mathbf{p}_J)^{\mathrm{T}}\right]^{\mathrm{T}}$ and $\{i_1, \cdots, i_M\} \in \mathcal{I}(\mathbf{p}_J)$. Substituting (41) into (43.a) and (43.b) and after some algebra the proof follows. ■

Theorem 4 provides sufficient conditions for the equivalence between the solutions of the SSR and of the EGOPA-OP, and, since (15) is convex, it also states the uniqueness condition for the QVI($\mathcal{K}, F$). Let us note that the sequence in which the J sub-problems are solved does not affect, in general, the optimality of the SSR solution, since it is sufficient for the partition of the set, no matter how obtained, to satisfy the optimality condition at the last increment. Unfortunately, there is no simple procedure to find the point-to-set map $\mathcal{K}(\delta\mathbf{p}^*)$ guaranteeing the optimality conditions. Hence, since the practical implementation of the SSR is viable only if the J-sized vector of power increments can be easily computed, in the next section we focus on a near-optimal criterion, referred to as *extreme points criterion*, to easily design the reduced subsets for all $j \in \mathcal{J}$.

E. Extreme Points Criterion

Let us assume that the values $\{\Theta_{j,n}\}_{n=1}^{N}$ identify the extreme points of the set, i.e., the maximum allowed power increment per each subcarrier that does not violate any of the constraint of the problem, regardless of the other subcarriers. These values are expressed by

$$\Theta_{j,n} \triangleq \min\left\{\bar{P}_{j,n}, \{\bar{I}_{j,l,n}\}_{l=1}^{L}, \bar{T}_{j,n}\right\}, \tag{44}$$

with

$$\bar{P}_{j,n} \triangleq P - \sum_{\nu=1}^{N} p_{j-1,\nu}, \tag{45}$$

$$\bar{I}_{j,l,n} \triangleq \left(I_l - \sum_{\nu=1}^{N} p_{j-1,\nu} K_{l,\nu} \right) / K_{l,n}, \quad 1 \leq l \leq L, \tag{46}$$

and

$$\bar{T}_{j,n} \triangleq T_{\phi(n)} - \sum_{\nu:\phi(\nu)=\phi(n)} p_{j-1,\nu}. \tag{47}$$

As apparent, the reduced set $\mathcal{K}_j$ is obtained by the intersection of the halfspace of the positive power increments with the halfspace lying below the hyperplane passing by the extreme points defined as $E_{j,n} \triangleq \{\overbrace{0, \cdots, 0}^{n-1}, \Theta_{j,n}, \overbrace{0, \cdots, 0}^{N-n}\}$, $\forall n \in \mathcal{D}_s$, properly shifted to take into account the partial solution $\mathbf{p}_j$ obtained so far. Figure 3 illustrates the extreme points criterion for a "toy" case with $N = 2$ subcarriers, $U = 2$ UPUs, with $\phi(1) = 1$ and $\phi(2) = 2$, and $L = 1$ IPU. The set delimited by the black thick line represents the set of feasible power values, identified by the intersection of constraints (15.a)-(15.b). The algorithm starts evaluating the first reduced set, consisting of the larger grey-shaded triangular-shaped area, and finds the first increment of power that belongs to the edge of this set. Then, the new reduced set is built by re-centering the origin of the axes on the previously found solution $\delta\mathbf{p}_1$ and evaluating the new extreme points. This second step evaluates then a new reduced set, consisting of the smaller grey-shaded triangular-shaped area, and proceeds again by finding the second increment of power $\delta\mathbf{p}_2$ that belongs to the edge of this new set. This procedure is iterated until the last increment lies on the initial set border. Some observations are now in order.

1) *Features*. The proposed SSR algorithm iteratively reduces the set of feasible power increments until, after J steps, no further power increment that would not violate any of the constraints is feasible, i.e., $\Theta_{J,n} = 0$, $\forall n \in \mathcal{D}_s$. However, in order to avoid possible cases where $J \to \infty$, a safer stop criterion was adopted, such that $||\mathbf{\Theta}_J|| \leq \epsilon_{\text{SSR}}$, where ϵ_{SSR} is a conveniently small value. In particular, at each step, the best local choice is performed solving the SSR subproblem (21). This problem is equivalent to the PA problem in [16], with the only difference that the constraint on the total available power is now replaced by the constraint of feasible power increments. In a way, the original constraints (15.b) are progressively dumped on $\Theta_{j,n}$, so that, at each step, the problem formulation is analogous to a non-cognitive case.

2) *Optimality*. Let us denote with $\tilde{\mathcal{N}}$ the set of subcarrier indices such that $\Theta_{J,n} > 0$ and assume that $\mathcal{I}(\mathbf{p}_J)$ is a singleton. Comparing equations (44)-(47) with (41), it can be noted that the SSR solution is optimal for those subcarriers that belong to $\tilde{\mathcal{N}}$. As a consequence, if $\mathbf{p}_{J-1}$ is an interior point of the original set, global optimality occurs whenever the set $\mathcal{I}(\mathbf{p}_J)$ is a singleton, i.e. every time that, at the optimal solution, only one constraint in (15.b) holds with equality. In this sense, we can claim that the SSR algorithm follows a *near optimality criterion*.

3) *Complexity*. Both the power increment $\delta\mathbf{p}_j$ and the parameters $\{\Theta_{j,n}, \tilde{\alpha}_{j,n}, \tilde{\rho}_{j,n}\},\ \forall n$, at each step j have a closed-form expression, so that the complexity of the algorithm simply reduces to $\mathcal{O}(J)$. The SSR algorithm is briefly summarized in the pseudo-code of Table II.

F. AMC-SSR Algorithm

As outlined in Sect. III, once the PA for a certain TM is evaluated, then the EGP is maximized performing a simple exhaustive search overall the possible TMs. Denoting with $\overline{m}^{(i)}$ the ith element of the set $\mathcal{D}_m$, this procedure, named AMC-SSR algorithm, is made of M steps and is summarized in Table III.

It is worth noting that this exhaustive approach is made possible thanks to the low complexity of the SSR algorithm that in J closed-form steps is able to evaluate the PA $\mathbf{p}^*(\boldsymbol{\varphi})$ for a given $\boldsymbol{\varphi}$. The advantage earned with the AMC approach is great: at each SNR, we are able to always choose the best setting of transmission parameters, so that the GP performance are always greater or equal than the ones obtained keeping a fixed TM.

VI. Simulation Results

In this section, the LRA method is numerically verified for realistic cognitive wireless scenarios. First, the SSR algorithm is checked against the LDD technique to ensure that, practically, both of them yield the same EGP performance. Then, the proposed AMC strategy based on the SSR algorithm is evaluated in terms of the actual GP (AGP) performance.

A. System Setup

Simulations have been carried out on a BIC-OFDM scenario, wherein each transmitted packet is made of $N_{\mathrm{p}} + N_{\mathrm{CRC}}$ bits, with $N_{\mathrm{p}} = 1024$ and $N_{\mathrm{CRC}} = 32$. The overall system RF bandwidth is $B_{\mathrm{tot}} = 20$ MHz with the central frequency of $f_0 = 2$ GHz, the subcarrier spacing is 15.152 kHz, the FFT size is 2048 and the cyclic prefix length is $1/4$ of the OFDM symbol interval. Channel encoding is based either on a 64-state convolutional code with mother code $r_0 = 1/2$ and $\mathcal{D}_r = \{1/2, 2/3, 3/4, 5/6\}$ or a turbo code with mother code $r_0 = 1/3$ and $\mathcal{D}_r = \{1/3, 2/5, 1/2, 4/7, 2/3, 3/4, 4/5, 6/7\}$. The set $\mathcal{D}_m$ is chosen to be $\{2, 4, 6\}$ corresponding to $4-$, $16-$ and $64-$QAM modulation, respectively. Thus, the total number of TMs is 12 when the convolutional code is employed and 24 under turbo code adoption. The channel is assumed to be static during each packet transmission, i.e., block-fading channel, and is identified by the 6-tap power profile of the ITU Pedestrian B model with path loss model specified by the COST231 Hata Model. The noise power level over the whole system band is -100 dBm and $P \in [0, 50]$ dBm.

The primary network considers U UPUs and L IPUs, transmitting over contiguous bands having the same size, i.e., $B_u = W_\ell = B_{\rm tot}/(L+U)$, $1 \leq u \leq U$, $1 \leq \ell \leq L$. As depicted in Fig. 4, the SR is placed at the origin of the reference system with the ST being 160 meters away. The IPUs are set round the secondary receiver within a radius of $R = 200$ meters, the UPUs are placed round the secondary receiver at a distance of at least 200 meters from it, according to the interference-free zone mentioned in Sect. II-C. The interference threshold, referred at the primary receivers, is set to I for all the UPUs and IPUs.

B. Validation of the SSR Algorithm

Figure 5 compares the optimum EGP, obtained with the LDD technique (empty circles) and the EGP produced by the SSR algorithm (full circles), versus the mean-available-symbol-energy-to-noise-spectral density ratio E_s/N_0 ratio at the SR, where E_s is evaluated assuming that all the available transmit power is employed. These results are obtained averaging 10^3 independent channel realizations, with the ST employing $N_{\rm tot} = 64$ subcarriers together with a convolutional encoder and static modulation and coding according to three different TMs, i.e., $\boldsymbol{\varphi}_1 \triangleq \{2, 3/4\}$, $\boldsymbol{\varphi}_2 \triangleq \{4, 1/2\}$ and $\boldsymbol{\varphi}_3 \triangleq \{6, 5/6\}$. The primary network is composed of $U = 1$ UPU and $L = 2$ IPUs, placed at 660, 85 and 52 meters from the ST, respectively. The interference temperature is $I = -110$ dBm. The LDD parameters are $\xi_m = \vartheta_m^{(0)}/10$, $0 \leq m \leq U + L + 1$, $\varepsilon = 10^{-4}$ and $I_{\max} = 10^6$.

For all the considered TMs, it is apparent that the SSR algorithm suffers a slight performance loss with respect to the LDD method, which can be appreciated for $\boldsymbol{\varphi}_2$ only, while it is negligible for all the other ones. The advantage we earn applying the SSR algorithm instead of conventional numerical methods is enlightened in Fig. 6, which depicts the number of iterations required to converge by the SSR (solid line), LDD (circles) and interior-point (squares), the latter for $\boldsymbol{\varphi}_4 \triangleq \{6, 2/3\}$, algorithms. We observe that the SSR algorithm needs less than 10 iterations to converge for any TM, the LDD method more than some orders of magnitude and the interior-point method about 50 outer iterations and, for each of them, an average of 10 inner iterations. Moreover, each iteration of the SSR is in closed-form, compared to the iterations of the interior-point method that are based on numerical algorithms, obtaining thus great saving in computational complexity.

Further, Fig. 7 shows the comparison between the EGP defined in (9) (empty marks) and the AGP (full marks), i.e., the average of the ratio between the number of information bits N_p and the time required to successfully deliver them, versus the E_s/N_0 ratio when the AMC-SSR algorithm is adopted. Both convolutional (squares) and turbo (circles) encoders are considered, with $N_{\rm tot} = 1320$ subcarriers, $U = 2$ UPUs and $L = 3$ IPUs at 400, 597, 85, 52 and 87 meters from the ST, respectively, and $I = -110$ dBm. It

can be seen how the EGP reliably works in predicting the actual link performance, exhibiting a normalized error that is always lower than 10%. Figure 7 also shows the benefit of adopting the AMC algorithm w.r.t. static TMs (dotted grey lines). As matter of fact, if the modulation order and coding rate were fixed, the system performance would incur in one of the following two cases: *i*) if a conservative TM were adopted, i.e., low modulation order and/or high coding rate, the performance would be good at low E_s/N_0, but would prematurely flatten out as the E_s/N_0 increases; ii) on the contrary, if more aggressive TM were employed, we would get low AGP values at low E_s/N_0 and good values only in medium-high E_s/N_0 region. The AMC algorithm instead always selects the best TM making the performance lie over the envelope determined by the static modes. The same behavior was obtained with turbo codes (not reported on the graph for the sake of clearness).

C. Goodput Performance of the AMC-SSR Algorithm

In Fig. 8 and 9, the AGP improvements brought forth by the AMC-SSR algorithm (full marks) are quantified for both convolutional and turbo encoding, respectively, when adopting as performance benchmark the same AMC algorithm based on a conventional SL-PA strategy, referred to as AMC-SL for short (empty marks), recently proposed in [7]. Simulations are carried out averaging 10^4 independent channel realizations, for $N_{\text{tot}} = 1320$, $U = 2$ UPUs and $L = 3$ IPUs, whose positions are randomly determined at each packet transmission according to the scenario in Fig. 4. Two different interference thresholds are considered (for UPUs, it is equivalent to change the radius of the interference-free zone), that is to say $I = -100$ dBm (squares), i.e. the same as the channel noise level, and $I = -110$ dBm (circles). The dashed curve tagged Non Cognitive Scenario stands for the AMC-SSR algorithm without any PU constraint, i.e., with $I = +\infty$. As such, this AMC scheme gives the best attainable AGP performance since it allocates all the available power and coincides with the scheme recently proposed in [16] for a non-cognitive scenario.

Both figures show that the proposed AMC-SSR algorithm outperforms the non-adaptive AMC-SL, enabling a maximum relative gain on the AGP of around 25% and 47% for $I = -100$ dBm and $I = -110$ dBm, respectively. The behavior shown by the AMC-SSR and AMC-SL algorithms can be readily explained as follows. In the low E_s/N_0 regime, the SU link performance is limited by the channel frequency selectivity rather than the interference caused to the PUs, which can be promptly neglected. The AMC-SSR is very close to the non-cognitive case with $I = +\infty$, indeed, and upon cleverly distributing the power over the subcarriers with the highest channel gains, it outperforms the non adaptive AMC-SL scheme. In the medium-to-high E_s/N_0 regime, instead, when the available power increases, the main constraint to satisfy turns out to be the interference caused to the PUs. Here, the SL strategy makes the AGP curve flatten out at lower

E_s/N_0 values as it inefficiently allocates power among the subcarriers to satisfy the interference constraints without any specific adaptivity. As result, the maximum interference level is prematurely met and no power increase is permitted. On the other side, the AMC-SSR algorithm properly shapes the PA distribution while accounting both for the current channel realization and the topology of the primary network, so that the link performance is significantly boosted. This observation is corroborated by the results obtained both in Fig. 8 and 9, when the interference threshold I decreases from -100 to -110 dBm. As a matter of fact, as the interference constraints get tighter, the AGP curves of the AMC-SL flattens out at lower and lower E_s/N_0 values compared with what we have with the proposed AMC-SSR algorithm.

VII. Concluding Remarks

In this paper, we addressed the LRA problem, i.e., modulation and coding scheme along with power-per-subcarrier, for a cognitive BIC-OFDM system. The resulting strategy is based upon the optimization of the goodput metric under constraints on the total power available at the secondary transmitter and the maximum interference tolerable at the primary receivers. First, we proved that the PA optimization problem is convex and its solution can be found exploiting conventional numerical methods. However, to overcome some critical drawbacks of these numerical solutions, such as the high computational complexity, the PA problem was re-interpreted through the QVI framework, which yielded the novel iterative SSR algorithm and allowed us to prove the existence and uniqueness of its solution. We also derived an optimum AMC procedure to further enhance the link performance. Simulation results corroborated the analytical derivation and showed that the proposed approach: *i*) gives, practically, identical goodput performance to that offered by the conventional numerical methods; *ii*) enables fast convergence making it extremely suitable for practical time-varying wireless scenarios; *iii*) has better actual average goodput performance over conventional non-adaptive PA algorithms.

Acknowledgment

This work was supported by the European Commission in the framework of the FP7 Network of Excellence in Wireless COMmunications NEWCOM# (Grant agreement no. 318306).

Part of the authors would like to thank the Belgium Federal Science Policy Office (BELSPO) for the support of the IAP BESTCOM network.

The authors would like also to thank the Associate Editor and the anonymous Reviewers for their constructive comments that contributed to improve the paper.

APPENDIX

A. Proof of Theorem 1

Let associate the Lagrange multipliers μ_n, $1 \leq n \leq N$, and ϑ_m, $0 \leq m \leq U+L$, to the inequality constraints (15.a) and (15.b), respectively, and cast them into $\boldsymbol{\eta} \triangleq [\mu_1, \cdots, \mu_N, \vartheta_0, \cdots, \vartheta_{U+L}]^{\mathrm{T}}$. Upon applying the KKT conditions, we obtain

$$\nabla_{\mathbf{p}} \psi(\mathbf{p}^*) + \boldsymbol{\vartheta}^{\mathrm{T}} \nabla_{\mathbf{p}} \boldsymbol{f}(\mathbf{p}^*) = 0, \tag{48}$$

$$\boldsymbol{\eta} \succeq \mathbf{0}, \tag{49}$$

$$\mu_n p_n^* = 0, \quad 1 \leq n \leq N, \tag{50}$$

$$\vartheta_m f_m(\mathbf{p}^*) = 0, \quad 0 \leq m \leq U+L. \tag{51}$$

Then, we obtain from (48), for $1 \leq n \leq N$,

$$-\frac{\alpha_n}{\rho_n} \mathrm{e}^{-p_n^*/\rho_n} - \mu_n + \vartheta_0 + \vartheta_{\phi(n)} + \sum_{l=1}^{L} \vartheta_{U+l} K_{l,n} = 0, \tag{52}$$

that, under (50), gives

$$\left(\vartheta_0 + \vartheta_{\phi(n)} + \sum_{l=1}^{L} \vartheta_{U+l} K_{l,n} - \frac{\alpha_n}{\rho_n} \mathrm{e}^{-p_n^*/\rho_n} \right) p_n^* = 0, \tag{53}$$

whereas, according to (49), we get

$$\vartheta_0 + \vartheta_{\phi(n)} + \sum_{l=1}^{L} \vartheta_{U+l} K_{l,n} \geq \alpha_n/\rho_n \mathrm{e}^{-p_n^*/\rho_n}. \tag{54}$$

Now, there exist two possible cases. First, when $\vartheta_0 + \vartheta_{\phi(n)} + \sum_{l=1}^{L} \vartheta_{U+l} K_{l,n} < \alpha_n/\rho_n$, then (54) is satisfied only if $p_n^* > 0$. This means that the optimal PA results from (53) as

$$p_n^* = \rho_n \left(\log \frac{1}{\vartheta_0 + \vartheta_{\phi(n)} + \sum_{l=1}^{L} \vartheta_{U+l} K_{l,n}} - \log \frac{\rho_n}{\alpha_n} \right). \tag{55}$$

Alternatively, the condition $\vartheta_0 + \vartheta_{\phi(n)} + \sum_{l=1}^{L} \vartheta_{U+l} K_{l,n} \geq \alpha_n/\rho_n$ is not allowed since if $p_n^* > 0$ it would violate (53) and so the only admissible value is $p_n^* = 0$. Hence, combining together these results the optimal PA over the nth subcarrier can be written

$$p_n^* = \rho_n \left[\log \frac{1}{\vartheta_0^* + \vartheta_{\phi(n)}^* + \sum_{l=1}^{L} \vartheta_{U+l}^* K_{l,n}} - \log \frac{\rho_n}{\alpha_n} \right]^+, \tag{56}$$

where $\boldsymbol{\vartheta}^*$ is the optimal value of the Lagrange multipliers. Finally, since the EGOPA-OP is convex, from the convex optimization theory it is known that the solution is also unique.

B. Proof of Closed Point-to-Set Mapping

For a given $j \in \mathcal{J}$ define, $\mathbf{z}^{(k)}(j) \triangleq [\mathbf{z}_1^{(k)}(j)^{\mathrm{T}}, \cdots, \mathbf{z}_l^{(k)}(j)^{\mathrm{T}}, \cdots, \mathbf{z}_J^{(k)}(j)^{\mathrm{T}}]^{\mathrm{T}}$ $\forall k$, where

$$\mathbf{z}_l^{(k)}(j) = \begin{cases} \delta\mathbf{v}_j^{(k)} & \text{if } \ l = j, \\ \delta\mathbf{p}_l^{(k)} & \text{otherwise.} \end{cases} \tag{57}$$

From (33) we have

$$\bar{\mathbf{z}}_l(j) \triangleq \lim_{k\to\infty} \mathbf{z}_l^{(k)}(j) = \begin{cases} \delta\bar{\mathbf{v}}_j, & \text{if } \ l = j, \\ \delta\bar{\mathbf{p}}_l, & \text{otherwise.} \end{cases} \tag{58}$$

For the sake of notation, from now on the dependence on j will be omitted. Thus, exploiting the assumption a) and b) and the convex nature of optimization problem (21), for each k, there exist two KKT multipliers $\lambda_j^{(k)}$ and $\mu_j^{(k)}$ such that the jth system

$$\begin{gathered} \nabla_{\delta\mathbf{p}_j}\psi_j(\mathbf{z}_j^{(k)}) + \lambda_j^{(k)}\nabla_{\delta\mathbf{p}_j} w_j(\mathbf{z}^{(k)}) + \mu_j^{(k)}\nabla_{\delta\mathbf{p}_j} u_j(\mathbf{z}_j^{(k)}) = 0 \\ \lambda_j^{(k)} \geq 0, \ \ \mu_j^{(k)} \geq 0, \ \ \mu_j^{(k)} u_j(\mathbf{z}_j^{(k)}) = 0, \ \ \lambda_j^{(k)} w_j(\mathbf{z}^{(k)}) = 0 \end{gathered} \tag{59}$$

is solved. Since the SBCQ is satisfied, we can claim that there always exist two bounded KKT multipliers $\bar{\lambda}_j$ and $\bar{\mu}_j$ such that

$$\lim_{k\to\infty} \lambda_j^{(k)} = \bar{\lambda}_j \quad \lim_{k\to\infty} \mu_j^{(k)} = \bar{\mu}_j. \tag{60}$$

Thus, for $k \to \infty$, $\delta\bar{\mathbf{v}}_j \in \mathcal{S}_j(\delta\bar{\mathbf{p}}_{-j})$, $\forall j \in \mathcal{J}$, as desired.

C. Proof of Theorem 3

The reduced set PA problem corresponds to the PA algorithm for EGP optimization proposed [16], where the constraint on the total available power is here substituted by constraint (21.c). Accordingly, this problem has a closed-form solution that is obtained as summarized in the following, where the dependence on the step j of the SSR algorithm is dropped w.l.g. Be $\delta\mathbf{p}^*$ the solution of the OP (21), its directional derivative must satisfy

$$(\delta\mathbf{p} - \delta\mathbf{p}^*)^{\mathrm{T}} \bigtriangledown \psi_j(\delta\mathbf{p}^*) = \sum_{n=1}^{N} (\delta p_n - \delta p_n^*) \left.\frac{\partial\psi_j(\delta\mathbf{p})}{\partial\delta p_n}\right|_{\delta\mathbf{p}=\delta\mathbf{p}^*} \geq 0, \tag{61}$$

which yields

$$\sum_{n=1}^{N} p_n \left.\frac{\partial\psi_j(\delta\mathbf{p})}{\partial\delta p_n}\right|_{\delta\mathbf{p}=\delta\mathbf{p}^*} \geq \sum_{n=1}^{N} \delta p_n^* \left.\frac{\partial\psi_j(\delta\mathbf{p})}{\partial\delta p_n}\right|_{\delta\mathbf{p}=\delta\mathbf{p}^*} \triangleq C. \tag{62}$$

Since (61) is an affine function of the power $\delta\mathbf{p}$, it can be evaluated on the N extreme points $\{\Theta_n\}_{n=1}^N$ of the set $\mathcal{D}_\Theta$ where, if $\delta p_n > 0 \ \forall n$, (62) holds with strict equality. Thus, setting $\delta p_k = \Theta_k$, with Θ_k given by

(44), and $\delta p_n = 0,\ \forall n \neq k$, in (62) we get the optimality condition

$$\Theta_k \left.\frac{\partial \psi_j(\delta \mathbf{p})}{\partial \delta p_k}\right|_{\delta \mathbf{p}=\delta \mathbf{p}^*} = C,\ \ \forall k,\ 1 \leq k \leq N. \tag{63}$$

This means that all the weighted components of the gradient of the objective function must be equal. Considering N active subcarriers, this condition can be obtained in N steps, where at the generic step i, with $i < N$, the current power $\delta p_k^{(i-1)}$ over all the subcarriers $k \leq i$ is increased of $\delta \tilde{p}_k^{(i)}$, i.e., $\delta p_k^{(i)} = \delta p_k^{(i-1)} + \delta \tilde{p}_k^{(i)}$, so that condition (63) is satisfied $\forall k \leq i+1$. In particular, defining

$$\delta \mathbf{p}^{(i)} \triangleq \left[\sum_{k=1}^{i} \delta \tilde{p}_1^{(k)}, \sum_{k=2}^{i} \delta \tilde{p}_2^{(k)}, \cdots, \delta \tilde{p}_i^{(i)}, \overbrace{0, \cdots, 0}^{N-i}\right]^{\mathrm{T}}, \tag{64}$$

from (62)

$$\Theta_1 \left.\frac{\partial \psi_j(\delta \mathbf{p})}{\partial \delta p_1}\right|_{\delta \mathbf{p}=\delta \mathbf{p}^{(i)}} = \cdots = \Theta_{i+1} \left.\frac{\partial \psi_j(\delta \mathbf{p})}{\partial \delta p_{i+1}}\right|_{\delta \mathbf{p}=\delta \mathbf{p}^{(i)}} \tag{65}$$

we get

$$\delta \tilde{p}_i^{(i)} = \rho_i \log\left(\frac{\tilde{\alpha}_i \tilde{\rho}_{i+1}}{\tilde{\rho}_i \tilde{\alpha}_{i+1}}\right)\ \ (\mathrm{a}),\ \ \frac{\delta \tilde{p}_k^{(i)}}{\rho_k} = \frac{\delta \tilde{p}_i^{(i)}}{\rho_i}\ \ \forall k \leq i\ \ (\mathrm{b}), \tag{66}$$

where $\tilde{\rho}_i \triangleq \frac{\rho_i}{\Theta_i}$. The last increment $\delta \tilde{p}_n^{(N)}$, $1 \leq n \leq N$, is such that constraint (21.a) holds with strict equality

$$\sum_{n=1}^{N} \left(\prod_{\substack{k=1 \\ k \neq n}}^{N} \Theta_k \delta \tilde{p}_n^{(N)}\right) + \sum_{i=1}^{N-1} \sum_{m=i}^{N-1} \left(\prod_{\substack{j=1 \\ j \neq i}}^{N} \Theta_j \delta \tilde{p}_i^{(m)}\right) = \prod_{i=1}^{N} \Theta_i. \tag{67}$$

Substituting $\delta \tilde{p}_n^{(N)} = \rho_n \frac{\delta \tilde{p}_N^{(N)}}{\rho_N}$ according to (66.b) into (67), $\delta \tilde{p}_N^{(N)}$ is obtained. Plugging its expression into

$$\delta p_n^* \triangleq \sum_{k=1}^{N} \delta \tilde{p}_n^{(k)} = \rho_n \left[\log\left(\frac{\tilde{\alpha}_n}{\tilde{\rho}_n}\right) - \log\left(\frac{\tilde{\alpha}_N}{\tilde{\rho}_N}\right)\right] + \rho_n \frac{\delta \tilde{p}_N^{(N)}}{\rho_N}, \tag{68}$$

the closed form (35) is eventually found.

REFERENCES

[1] J. M. III and G. M. Jr., "Cognitive radio: making software radios more personal," *IEEE Pers. Commun.*, vol. 6, no. 4, pp. 13 –18, Aug. 1999.

[2] S. Haykin, "Cognitive radio: brain-empowered wireless communications," *IEEE J. Sel. Areas in Commun.*, vol. 23, no. 2, pp. 201 – 220, Feb. 2005.

[3] FCC, "Second report and order and memorandum opinion and order," U. S. Federal Communications Commission, Tech. Rep. FCC 08-260, 2008.

[4] A. Goldsmith, S. Jafar, I. Maric, and S. Srinivasa, "Breaking spectrum gridlock with cognitive radios: An information theoretic perspective," *Proceedings of the IEEE*, vol. 97, no. 5, pp. 894 –914, May 2009.

[5] Z. Tian, G. Leus, and V. Lottici, "Joint dynamic resource allocation and waveform adaptation for cognitive networks," *IEEE J. Sel. Areas in Commun.*, vol. 29, no. 2, pp. 443 –454, Feb. 2011.

[6] R. Zhang and Y.-C. Liang, "Exploiting multi-antennas for opportunistic spectrum sharing in cognitive radio networks," *IEEE J. Sel. Topics Signal Processing*, vol. 2, no. 1, pp. 88 –102, Feb. 2008.

[7] G. Bansal, M. Hossain, and V. Bhargava, "Optimal and suboptimal power allocation schemes for ofdm-based cognitive radio systems," *IEEE Trans. on Wireless Commun.*, vol. 7, no. 11, pp. 4710 –4718, Nov. 2008.

[8] Z. Hasan, G. Bansal, E. Hossain, and V. Bhargava, "Energy-efficient power allocation in ofdm-based cognitive radio systems: A risk-return model," *IEEE Trans. on Wireless Commun.*, vol. 8, no. 12, Dec. 2009.

[9] P. Cheng, Z. Zhang, H.-H. Chen, and P. Qiu, "Optimal distributed joint frequency, rate, and power allocation in cognitive ofdma systems," *IET Comm.*, vol. 2, no. 6, pp. 815–826, July 2008.

[10] Y. Ma, D. I. Kim, and Z. Wu, "Optimization of ofdma-based cellular cognitive radio networks," *IEEE Trans. on Commun.*, vol. 58, no. 8, pp. 2265 –2276, Aug. 2010.

[11] G. Caire, G. Taricco, and E. Biglieri, "Bit-interleaved coded modulation," *IEEE Trans. on Inf. Theory*, vol. 44, no. 3, pp. 927 –946, May 1998.

[12] S. Lin, D. Costello, and M. Miller, "Automatic-repeat-request error-control schemes," *IEEE Commun. Mag.*, vol. 22, no. 12, pp. 5 –17, Dec. 1984.

[13] A. Goldsmith and S.-G. Chua, "Variable-rate variable-power mqam for fading channels," *IEEE Trans. on Commun.*, vol. 45, no. 10, pp. 1218 –1230, Oct. 1997.

[14] D. Qiao, S. Choi, and K. Shin, "Goodput analysis and link adaptation for ieee 802.11a wireless lans," *IEEE Trans. on Mobile Comput.*, vol. 1, no. 4, pp. 278 – 292, Oct.-Dec. 2002.

[15] B. Devillers, J. Louveaux, and L. Vandendorpe, "Bit and power allocation for goodput optimization in coded parallel subchannels with arq," *IEEE Trans. on Signal Process.*, vol. 56, no. 8, pp. 3652 –3661, Aug. 2008.

[16] I. Stupia, V. Lottici, F. Giannetti, and L. Vandendorpe, "Link resource adaptation for multiantenna bit-interleaved coded multicarrier systems," *IEEE Trans. on Signal Process.*, vol. 60, no. 7, pp. 3644 –3656, July 2012.

[17] Y. Blankenship, P. Sartori, B. Classon, V. Desai, and K. Baum, "Link error prediction methods for multicarrier systems," in *IEEE 60th Vehicular Tech. Conf., 2004. VTC2004-Fall.*, vol. 6, Sept. 2004, pp. 4175 – 4179.

[18] L. Ruan and V. Lau, "Power control and performance analysis of cognitive radio systems under dynamic spectrum activity and imperfect knowledge of system state," *IEEE Trans. on Wireless Commun.*, vol. 8, no. 9, Sept. 2009.

[19] S. Boyd and L. Vandenberghe, *Convex Optimization*. Cambridge University Press, 2004.

[20] P. Tsiaflakis, I. Necoara, J. Suykens, and M. Moonen, "Improved dual decomposition based optimization for dsl dynamic spectrum management," *IEEE Trans. on Signal Process.*, vol. 58, no. 4, pp. 2230 –2245, Apr. 2010.

[21] F. Facchinei and J. Pang, *Finite-Dimensional Variational Inequalities and Complementary Problem*, 9th ed. New York, NY: Springer-Verlag, 2003.

[22] J.-S. Pang and M. Fukushima, "Quasi-variational inequalities, generalized nash equilibria, and multi-leader-follower games," *Computational Management Science*, 2005.

[23] Z.-Q. Luo, J.-S. Pang, and D. Ralph, *Mathematical Programs with Equilibrium Constraints*. Cambridge University Press, 1996.

[24] I. Stupia, L. Vandendorpe, R. Andreotti, and V. Lottici, "A game theoretical approach for coded cooperation in cognitive radio networks," in *Proc. of 5th Int. Symp. on Commun. Control and Signal Process. (ISCCSP), 2012*, May 2012, pp. 1 –6.

[25] I. Stupia, R. Andreotti, V. Lottici, and L. Vandendorpe, "A consensus approach for cooperative communications in cognitive radio networks," in *Proc. of the 20th European Signal Process. Conf. (EUSIPCO), 2012*, Aug. 2012, pp. 2674 –2678.

[26] W. W. Hogan, "Point-to-set maps in mathematical programming," *SIAM Review*, vol. 15, pp. 591–603, July 1973.

Initialize $i = -1$, $\mathbf{p}^{(0)} = \mathbf{p}_0$

Do

$i \leftarrow i + 1$

S1: Compute $\boldsymbol{\vartheta}^{(i+1)} = \left[\boldsymbol{\vartheta}^{(i)} + \boldsymbol{\xi}^{\mathrm{T}} \cdot \nabla \Lambda_{\boldsymbol{\vartheta}}(\boldsymbol{\vartheta}^{(i)}, \mathbf{p}^{(i)})\right]^{+}$

S2: Compute $\mathbf{p}^{(i+1)} = \inf_{\mathbf{p} \in \mathcal{D}_{\boldsymbol{p}}} \Lambda(\boldsymbol{\vartheta}^{(i+1)}, \mathbf{p})$

While $\left(||\mathbf{p}^{(i+1)} - \mathbf{p}^{(i)}|| > \epsilon\right)$ and $(i < I_{\max})$

Output $\mathbf{p}^{*} = \mathbf{p}^{(i)}$

TABLE I: Pseudo-code of the subgradient-based EGOPA-OP

Initialize $j = 1$, $\Delta\mathbf{p}^{(0)} = \mathbf{0}$

Do

$j \leftarrow j + 1$

Evaluate $\mathbf{p}_j$, $\boldsymbol{\Theta}_j$, $\{\tilde{\alpha}_{j,n}, \tilde{\rho}_{j,n}\}$ $\forall n$

Evaluate $\delta\mathbf{p}_j$ according to (35)

While $(||\boldsymbol{\Theta}_j|| > \epsilon_{\mathrm{SSR}})$

Set $J = j$

Output $\mathbf{p}^{*} = \sum_{j=1}^{J} \delta\mathbf{p}_j$

TABLE II: Pseudo-code of the SSR algorithm

Initialize $\zeta^{(0)} = 0$

For i=1:M

- Set $m^{(i)} = \overline{m}^{(i)}$
- Evaluate $\mathbf{p}^{(i)}$ and $\gamma^{(i)}$
- Enter $\gamma^{(i)}$ into the LUT and return the coding rate $r^{(i)}$ associated to the best EGP value $\zeta^{(i)}$
- If $\left(\zeta^{(i)} > \zeta^{(i-1)}\right)$

  Set $\mathbf{p}^* = \mathbf{p}^{(i)}$, $m^* = m^{(i)}$, $r^* = r^{(i)}$

End For

Output $(\mathbf{p}^*, m^*, r^*)$

TABLE III: Pseudo-code of the AMC-SSR algorithm

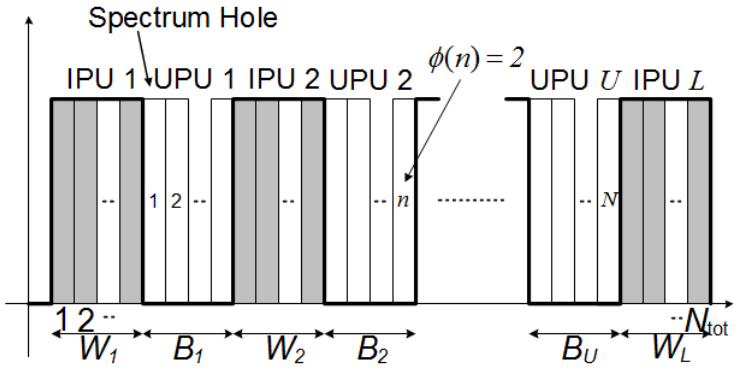

Fig. 1: Spectrum activity

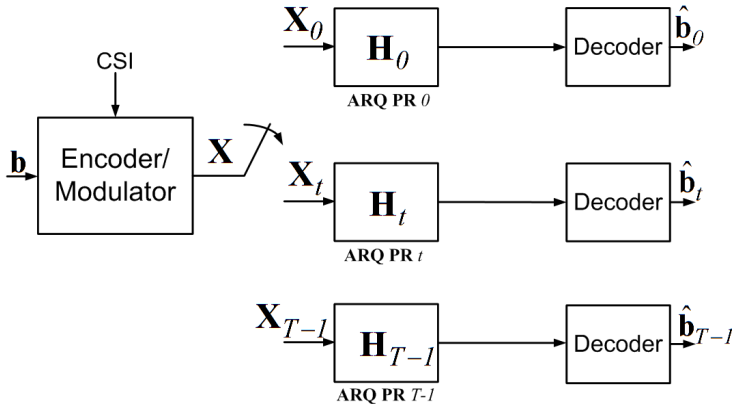

Fig. 2: Equivalent ARQ-based BIC-OFDM model

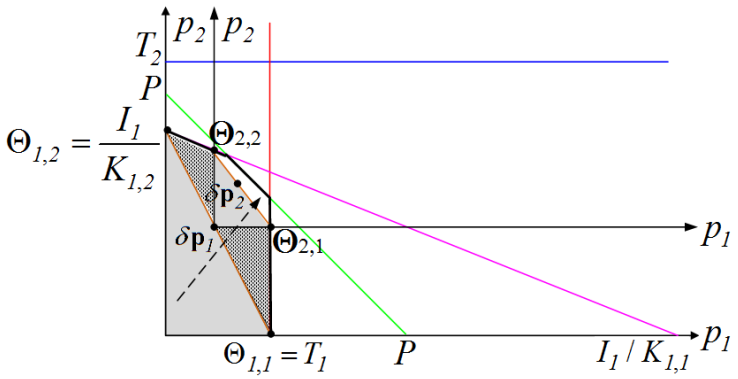

Fig. 3: Graphical interpretation of the extreme points criterion.

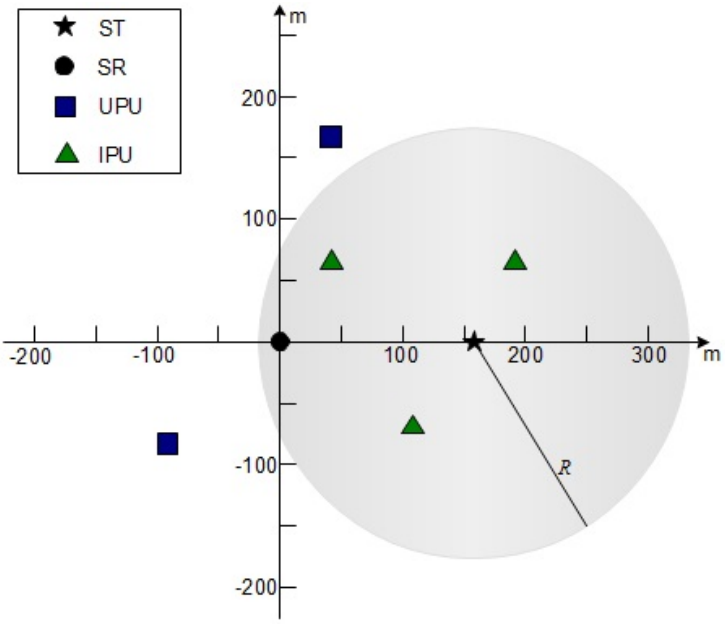

Fig. 4: Simulation scenario. Example with $U = 2$, $L = 3$.

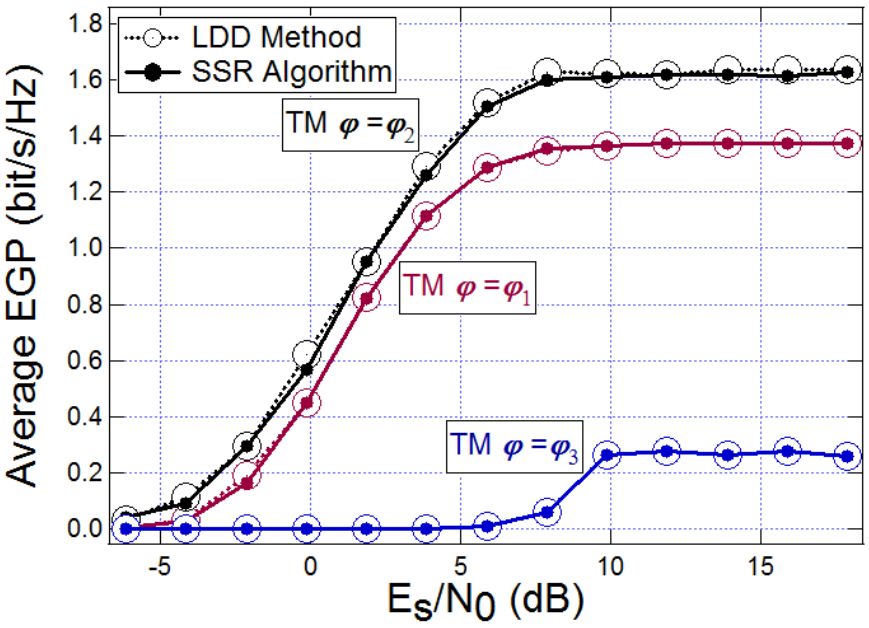

Fig. 5: LDD vs. SSR algorithm. Performance comparison.

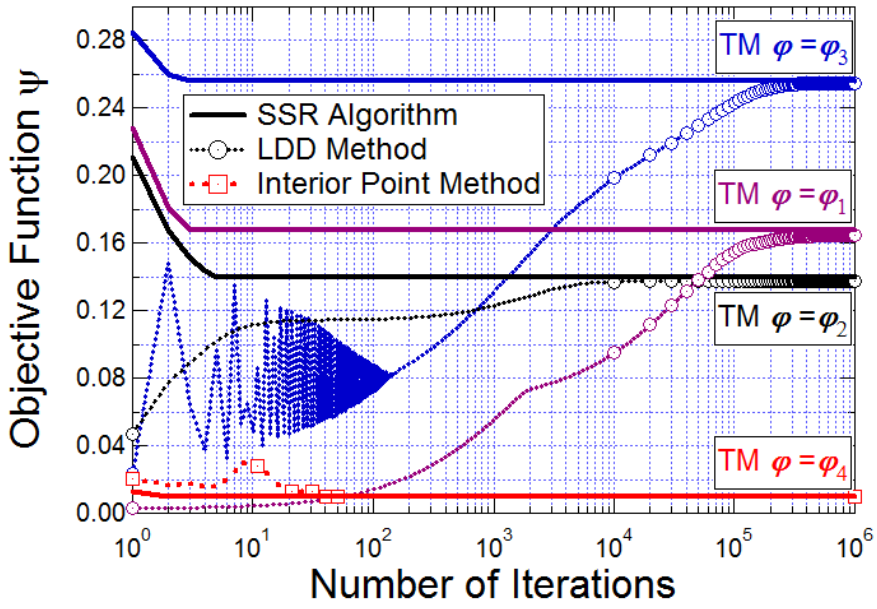

Fig. 6: LDD vs. SSR algorithm. Convergence comparison.

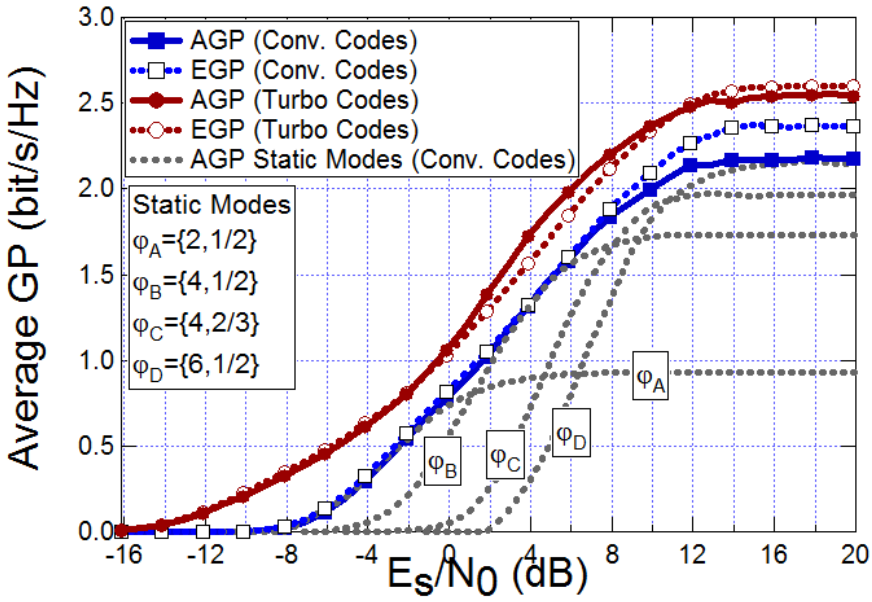

Fig. 7: Estimated vs. actual goodput comparison.

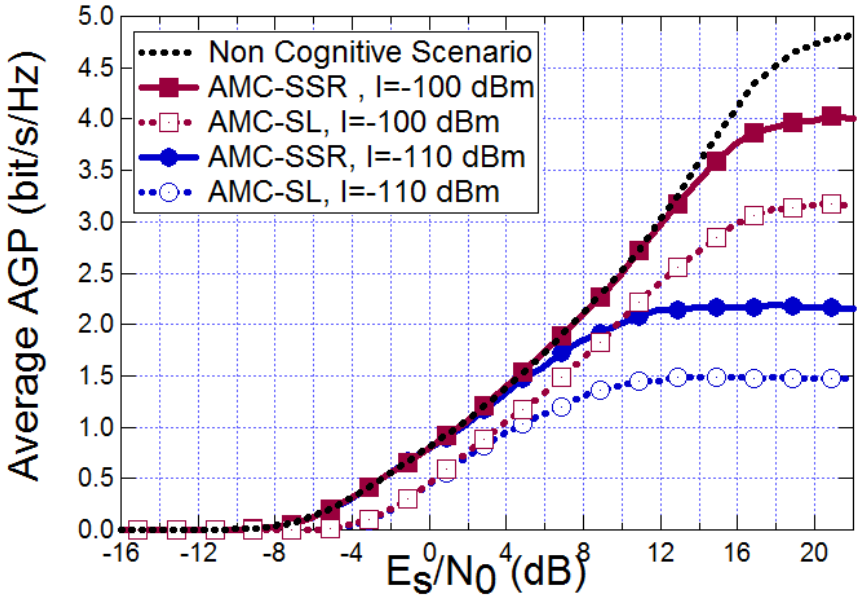

Fig. 8: AMC-SSR vs. AMC-SL algorithm. Performance comparison with convolutional codes.

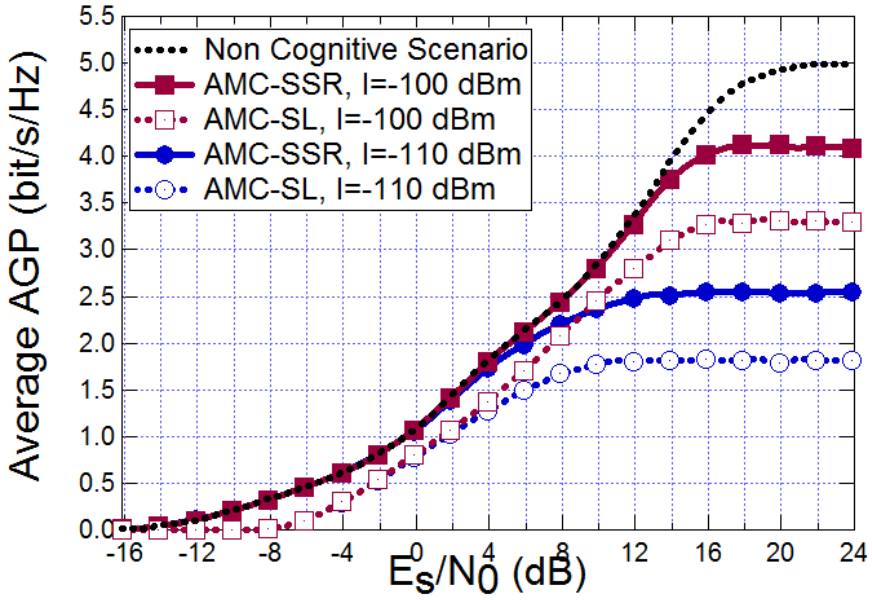

Fig. 9: AMC-SSR vs. AMC-SL algorithm. Performance comparison with turbo codes.